

**Antimicrobial nanocoatings onto the  
polymeric material to avoid hospital  
acquired infections.**



**By  
Tahreem Arshad**

**School of Chemical and Materials Engineering  
National University of Sciences and Technology  
2023**

# **Antimicrobial nanocoatings onto the polymeric material to avoid hospital acquired infections.**



Tahreem Arshad

Reg.No.00000327527

**This thesis is submitted as a partial fulfillment of the requirements  
for the degree of**

**“Master of Science (MS) in Nanoscience and Engineering”**

**Supervisor Name: Dr. Usman Liaqat**

**School of Chemical and Materials Engineering (SCME)**

**National University of Sciences and Technology (NUST)**

**H-12 Islamabad, Pakistan**

**January, 2023**



### THESIS ACCEPTANCE CERTIFICATE

Certified that final copy of MS thesis written by Ms Tahreem Arshad (Registration No 000003317527), of School of Chemical & Materials Engineering (SCME) has been vetted by undersigned, found complete in all respects as per NUST Statues/Regulations, is free of plagiarism, errors, and mistakes and is accepted as partial fulfillment for award of MS degree. It is further certified that necessary amendments as pointed out by GEC members of the scholar have also been incorporated in the said thesis.

Signature: \_\_\_\_\_

Name of Supervisor: Dr Usman Liaqat

Date: 04.09.23

Signature (HOD): \_\_\_\_\_

Date: 5/9/23

Signature (Dean/Principal): \_\_\_\_\_

Date: 6-9-2023

*Thesis submission certificate by Library ?*



136-07-2019

Form TH-1  
(Must be type written)

National University of Sciences & Technology (NUST)  
MASTER'S THESIS WORK

Formulation of Guidance and Examination Committee (GEC)

Name: TAHREEM ARSHAD NUST Regn No: 00000317527  
Department: SCME Specialization: NSF  
Credit Hour Completed: 24 CGPA: 3.13

Course Work Completed

S/No	Code	Title	Core/Elective	CH	Grade
1	MSE-952	Materials for Biomedical Applications	E	3	B+
2	NSE 441	Nano Composite Materials	E	3	B+
3	NSE-847	Essentials of NEMS and MEMS	E	3	B
4	MSE-872	Composite Materials	E	3	B
5	MSE-856	Nano materials and Processing	C	3	B+
6	NSE-845	Nanolithography And Device Fabric	E	3	B
7	NSE-813	Essentials of Nanoscience and Engineering	C	3	B
8	MSE-854	Characterization of Materials	C	3	C+

Date: 28-09-2021 Student's Signature: Tahreem Arshad Add Research methodology Exam Br ✓  
16/9/21

Thesis Committee

- Name: Dr. Usman Liaqat (Supervisor) Signature: [Signature]  
Department: Material Engineering
- Name: Dr. Zakir Hussain (Co-Supervisor) Signature: [Signature]  
Department: Materials Engineering
- Name: Dr. M. Bilal Khan Niazi Signature: [Signature]  
Department: Chemical Engineering
- Name: Dr. M. Aftab Akram Signature: [Signature]  
Department: Material Engineering
- Name: Dr. Mohsin Raza (External) Signature: [Signature]  
Department: DESTO, NESCOM

Date: 28/9/2021 Signature of Head of Department: [Signature]

APPROVAL

Date: 28.9.2021 [Signature]  
Dean/Principal

Distribution

- 1x copy to Exam Branch, Main Office NUST
- 1x copy to PGP Dte, Main Office NUST
- 1x copy to Exam branch, respective institute





National University of Sciences & Technology (NUST)

FORM TH-4

MASTER'S THESIS WORK

We hereby recommend that the dissertation prepared under our supervision by  
Regn No & Name: 00000317527 Tahreem Arshad


Title: Antimicrobial nanocoatings on the polymeric material to avoid hospital acquired  
infections.

Presented on: 17 Aug 2023 at: 1430 hrs in SCME (Seminar Hall)

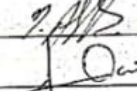
Be accepted in partial fulfillment of the requirements for the award of Masters of Science  
degree in Nanoscience & Engineering.

Guidance & Examination Committee Members

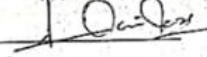
Name: Dr Muhammad Bilal Khan Niazi

Signature: 


Name: Dr Muhammad Aftab Akram

Signature: 

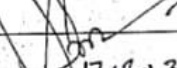
Name: Dr Mohsin Raza (External)

Signature: 

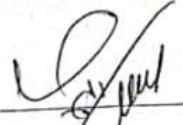
Name: Dr Zakir Hussain (Co-Supervisor)

Signature: 

Supervisor's Name: Dr Usman Liaqat

Signature: 

Dated: 17-8-23

  
Head of Department  
Date 20/8/23

  
Dean/Principal

Date 29.8.2023

School of Chemical & Materials Engineering (SCME)

## *Dedication*

*This thesis is dedicated to my parents for their love, support, sacrifices, prayers, and advice.*

## **Acknowledgements**

First and foremost, praises and thanks to ALLAH Almighty for the blessings he bestowed upon me, gave me strength, good health, and the ability to learn and understand to complete this research successfully. It is a genuine to express my deep and sincere gratitude to my honorable supervisors Prof. Dr Zakir Hussain and Prof. Dr Usman Liaqat, the best mentor, for sharing his experience and wealth of knowledge through his kind supervision, valuable guidance, and timely and constructive advice which helped me extensively in accomplishing my research work. Besides my supervisor, I thank profusely my Guidance and Examination Committee (GEC) members Dr. Bilal Khan Niazi and Dr. Muhammad Aftab Akram, and my fellow lab mates for the guidance, timely suggestions, and effective working environment. I owe a deep sense of appreciation to the lab technicians/engineers for the characterization of samples and assistance in understanding the instrumentations. I also acknowledge the help provided by fellows from the other labs. In addition, I would like to extend my sincere thanks to my best friends for their ceaseless cooperation and support both in and outside the lab throughout my research. I would like to convey my wholehearted gratitude to all the teachers/lecturers I learned from since childhood and everyone who has directly or indirectly helped me throughout my academic journey. Last but not the least, huge thanks to my parents and siblings for their unparalleled love, care, encouragement, financial and emotional support, and lots of prayers.

**Tahreem Arshad**

## Abstract

Bactericidal infections on medical implants are the main cause of hospital acquired infections which can be prevented by using antibacterial coatings onto the biomaterial surfaces. Various nanomaterials and their derived composites have recently been explored to be used as antibacterial agents. Likewise, in this study silver nanoparticles (NPs), zinc oxide nanoparticles (NPs), graphene oxide (GO) nanocomposites were synthesized through In-situ method. The synthesized nanocomposite was coated onto a polymeric material (silicone rubber) through the surface treatment of the required polymer. Which were further characterized by the following characterization techniques viz, SEM, EDS, FTIR, Raman, UV-Vis and XRD. These synthesized materials as well as the coated thin films were then investigated against Gram-negative (G<sup>-</sup>) bacteria *Escherichia coli* (*E. coli*) and the Gram-positive (G<sup>+</sup>) bacteria *Staphylococcus aureus* (*S. aureus*). GO-Ag-ZnO exhibits potential antibacterial and antiadhesive properties for use as antimicrobial coatings against bacterial adhesion and biofilm formation on silicone urinary catheters. The antibacterial activity was assessed by measuring the diameter of zone inhibition by determining the MIC and MBC.



# Table of Contents

Introduction.....	1
1.1. Urinary Catheters .....	1
1.1.1. Catheter associated Urinary tract infections (CAUTI).....	2
1.1.2. Classification of urinary catheter .....	2
1.1.3. Methods for Limiting CAUTI with Antibacterial Coatings.....	4
1.2. Brief description of this study .....	5
1.3. Objectives .....	6
2. Literature Review .....	7
2.1. Nanotechnology.....	7
2.1.1. Introduction.....	7
2.1.2. Synthesis of nanoparticles.....	7
2.2. Nanoparticles as antibacterial agents.....	8
2.2.1. Silver nanoparticles.....	9
2.2.2. Zinc Oxide nanoparticles .....	12
2.2.3. Graphene based nanomaterials GBNs.....	15
2.3. Nanomaterials based composites.....	18
3. Methodology.....	21
3.1. Chemicals and Materials .....	21
3.2. Ag NPs synthesis.....	21
3.3. ZnO NPs synthesis .....	22
3.4. Synthesis of In-situ nanocomposite.....	23
3.5. Synthesis of Graphene oxide GO its nanocomposites.....	23
3.6. Graphene oxide synthesis .....	24
3.7. Synthesis of GO-Ag, GO-ZnO, GO-Ag-ZnO nanocomposite through in-situ method:.....	25
3.7.1. GO-ZnO synthesis.....	25

3.7.2.	Synthesis of GO-Ag .....	25
3.7.3.	GO-Ag-ZnO nanocomposite synthesis .....	26
3.8.	Thin film preparation onto silicone rubber.....	27
3.8.1.	Cleaning of Silicone rubber .....	27
3.8.2.	Deposition of thin film via In-situ synthesis for Ag NPs.....	27
3.8.3.	Deposition of thin film via spin coating for GO-ZnO-Ag .....	28
3.9.	Characterization techniques.....	28
3.9.1.	X-ray Diffraction (XRD).....	28
3.9.2.	Working Principle of XRD .....	28
3.10.	Fourier Transform Infrared (FT-IR) spectroscopy .....	30
3.10.1.	Working Principle of FT-IR .....	30
3.11.	Scanning Electron Microscope (SEM) .....	29
3.11.1.	Working principle of SEM .....	29
3.12.	UV-Vis Spectroscopy .....	30
3.13.	Microbial culture.....	31
3.14.	Antibacterial activity measurement .....	31
3.15.	Optical imaging.....	32
3.16.	Contact angel measurement.....	32
3.17.	Plasma treatment.....	33
4.	Results and Discussion .....	34
4.1.	Instrumentation and measurements .....	34
4.2.	Scanning Electron Microscopy (SEM).....	34
4.3.	Energy-dispersive X-ray spectroscopy (EDS) .....	36
4.4.	X-ray diffraction (XRD).....	39
4.5.	Fourier transform infra-red (FT-IR) spectroscopy.....	41
4.6.	UV- Vis spectroscopy .....	42
4.7.	Contact angle measurement.....	44

4.8. Antibacterial activity of synthesized materials.....	45
4.8.1. Agar dilution method .....	45
4.8.2. Minimum inhibitory concentration MIC determination .....	50
4.8.3. Minimum bactericidal concentration MBC determination .....	50
Conclusion .....	52
References .....	53

## Table of Figures

Figure 1. 1. Indwelling urinary catheter.....	1
Table 1. 1. Comparison of the advantages and disadvantages of the materials used for urinary catheters.....	3
Figure 1.....	5
Figure 1. 2. Shows the possible multiple action of inorganic antibacterial agents against pathogenic microbes. ....	5
Figure 2. 1. Different methods of combining antibacterial agents with biomaterials..	8
Table 2. 1. Comparison of the antibacterial studies performed on AgNPs.....	11
Table 2. 2. Comparison of the antibacterial studies performed on ZnO NPs .....	14
Table 2. 3. Comparison of the antibacterial studies against GO.....	17
Table 2. 4. Comparison of the antibacterial studies performed on GBN based nanocomposites.....	20
Figure 3. 1. Synthesis of AgNPs .....	22
Figure 3. 1 Synthesis of AgNPs .....	22
Figure 3. 2. Synthesis of ZnO NPs.....	23
Figure 3. 3. Synthesis of Ag-ZnO nanocomposite.....	23
Figure 3. 4. Synthesis of Graphene oxide .....	24
Figure 3. 5. Synthesis of GO-ZnO nanocomposite .....	25
Figure 3. 6. Synthesis of GO-Ag nanocomposite .....	26
Figure 3. 7. Synthesis of GO-Ag-ZnO nanocomposite.....	27
Figure 3. 8. Contact angle measurement.....	33
Figure 4. 1. SEM images of a) silver nanoparticles b) Zinc oxide nanoparticles c) Graphene oxide d) Ag-ZnO e) GO-Ag f) GO-ZnO g) GO-Ag-ZnO nanocomposite.....	35
Figure 4. 2. Shows the SEM images of AgNPs coated silicone rubber at higher resolution.....	36
Figure 4. 3. EDS of silver nanoparticles .....	36
Figure 4. 5. EDS of graphene oxide GO .....	37
Figure 4. 6. EDS of GO-Ag nanocomposite .....	37
Figure 4. 4. EDS of zinc oxide nanoparticles ZnO NPs .....	37
Figure 4. 9. EDS of GO-Ag-ZnO nanocomposite .....	38
Figure 4. 8. EDS of Ag-ZnO nanocomposite.....	38

Figure 4. 7. EDS of GO-ZnO nanocomposite.....	38
Figure 4. 10. XRD pattern observed for AgNPs, ZnONPs and GO .....	40
Figure 4. 11. XRD pattern observed for the respective synthesized nanocomposites. .....	40
Figure 4. 12. XRD pattern of Bare silicone rubber, In-situ AgNPs coated silicone rubber and AgNPs.....	41
Figure 4. 13. FT-IR spectra of, Ag NPs, ZnO NPs and Graphene oxide GO .....	42
Figure 4. 14. FT-IR spectra of the synthesized nanocomposites. ....	42
Figure 4. 16. UV-Vis spectrum of the synthesized nanocomposite.....	43
Figure 4. 15. UV-Vis spectrum of AgNPs, ZnONPs and graphene oxide.....	43
Figure 4. 17. Contact angle measurement of a) bare silicone rubber b) Silver coated silicone rubber c) GO-Ag-ZnO nanocomposite coated silicone rubber.....	44
Table 4. 1 ZOI values of Ag, ZnO, GO, sample 1, sample 2, sample 3 and GO-Ag- ZnO nanocomposite against G+ and G- bacterial strains.....	46
Table 4. 2 ZOI values of Ag, ZnO, GO, sample 1, sample 2, sample 3 and GO-Ag- ZnO nanocomposite against G+ and G- bacterial strains.....	47
Figure 4. 18. Zone of inhibition values of Ag, ZnO, GO, sample 1, sample 2, sample 3 and GO-Ag-ZnO nanocomposite against <i>S. aureus</i> . ....	48
Figure 4. 19. ZOI values of Ag, ZnO, GO, sample 1,, sample 2, sample 3 and GO-Ag- ZnO nanocomposite against <i>E.coli</i> .....	49
Table 4. 3. Ag NPs and GO-Ag-ZnO nanocomposite MIC and MBC values .....	51
Table 4. 4. Ag NPs and GO-Ag-ZnO nanocomposite MIC and MBC values .....	51

## Table of Tables

Table 4. 1 ZOI values of Ag, ZnO, GO, sample 1, sample 2, sample 3 and GO-Ag-ZnO nanocomposite against G+ and G- bacterial strains.....	46
Table 4. 2 ZOI values of Ag, ZnO, GO, sample 1, sample 2, sample 3 and GO-Ag-ZnO nanocomposite against G+ and G- bacterial strains.....	47
Table 4. 3. Ag NPs and GO-Ag-ZnO nanocomposite MIC and MBC values .....	51
Table 4. 4. Ag NPs and GO-Ag-ZnO nanocomposite MIC and MBC values .....	51
Table 2. 1. Comparison of the antibacterial studies performed on AgNPs.....	11
Table 2. 2. Comparison of the antibacterial studies performed on ZnO NPs .....	14
Table 2. 3. Comparison of the antibacterial studies against GO.....	17
Table 2. 4. Comparison of the antibacterial studies performed on GBN based nanocomposites. ....	20

## List of Abbreviations

<b>CAUTI</b>	Catheter associated urinary tract infections
<b>AgNPs</b>	Silver nanoparticles
<b>ZnONPs</b>	Zinc Oxide nanoparticles
<b>GO</b>	Graphene Oxide
<b>E. coli</b>	Escherichia coli
<b>S. aureus</b>	Staphylococcus aureus
<b>GBNs</b>	Graphene based nanomaterials
<b>G+</b>	Gram positive
<b>G-</b>	Gram negative
<b>DI</b>	Deionized water
<b>NC</b>	Nanocomposite
<b>WCA</b>	Water contact angle
<b>Sample 1</b>	Ag-ZnO
<b>Sample 2</b>	GO-Ag
<b>Sample 3</b>	GO-ZnO



# Chapter 1

## Introduction

### 1.1. Urinary Catheters

The modern medical devices have advanced in recent years, in terms of treating and assisting people with chronic or life-threatening diseases. Despite being popular and being used in many fields, these medical devices expose the person to various infections. The most used invasive medical device is the Indwelling urinary catheters (IUC) [1]. Their main purpose is urine drainage, whether it's the temporary or permanent removal of urine from the bladder. Worldwide, more than 200 million urinary catheters are supplied, still the rate of catheterization remain high at 20% in non-intensive care units (ICUs) and 61% in intensive care units (ICUs) [2, 3]. The most common conditions for which these IUC are used in patients that are in coma, incontinence, have any injury related to spinal cord or nervous system, obstruction in urine flow and in patients with urine retention [4]. Patients who will be receiving anesthesia or sedation for the medical procedures such as cesarean sections, orthopedic procedures and any kind of operations in which patients' recovery requires them to have these urinary catheters [5]. Unfortunately, the rate of catheter associated infections increases by 2-6% everyday because of the installation of the urinary catheter. Around 50% of the patients develop catheter associated bacteriuria after 5-10 days of the insertion of urinary catheter [6].

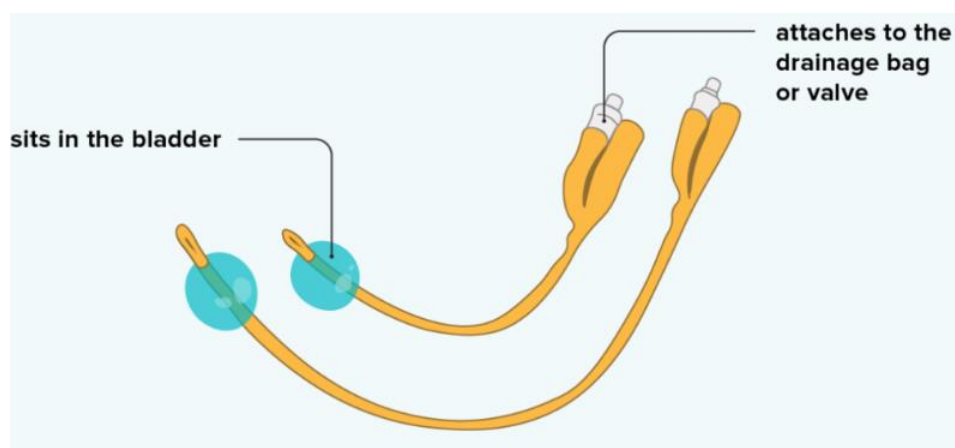


Figure 1. 1. Indwelling urinary catheter.

### **1.1.1. Catheter associated urinary tract infections (CAUTI)**

A significant risk to the health of public is due to the catheter associated urinary tract infections (CAUTIs) which accounts for 30-40% of them and cause bloodstream infectious with 30% fatality rate [7, 8]. *Escherichia coli*, *Pseudomonas aeruginosa*, *Staphylococcus* species, *Proteas mirabilis*, *Klebsiella pneumoniae*, *Proteus vulgaris*, Enterococcal species and fungi like *Candida albicans* are few of the bacterial species that can cause CAUTIs. The growth of such pathogenic microbes onto the urinary catheter can be prevented by coating or integrated with an antimicrobial substance which can act as antifouling agents or may be bactericidal/bacteriostatic. To prevent and manage CAUTIs some efforts have been made, by minimizing the dwell time and reducing its usage [9]. However, despite all these preventive measures, managing CAUTIs is difficult since microbial pathogens can form biofilms. When bacteria attach itself to the surface of solid it secretes protein matrices like deoxyribonucleic acid (DNA) and others, they form a complex community known as biofilm. Free-floating or planktonic bacteria will quickly attach themselves to the surface that is immersed in the fluid and within minutes they attach themselves. Bacteria when attached to the surface produce slimy, polymeric substances that are extracellular (EPS) which invade the surface and create the conditioning film. Due to the emergence of extracellular polymeric substances, it enables biofilm causing bacteria to construct a complex, 3-D structure that is influenced by a range of external influences. According to reports, biofilms typically have a thickness of 200  $\mu\text{m}$  but can occasionally reach 500  $\mu\text{m}$ . How rapidly the bacteria attach itself to the catheter depends upon the quantity and the type of bacteria present in the urine or the surroundings to which the catheter is exposed, the rate of liquid flow, and the physicochemical properties of catheter's surface. Biofilm formation is one of the major causes of chronic infections. It protects pathogenic bacteria against antibiotics.

### **1.1.2. Classification of urinary catheter**

Standard urinary catheters are made from a variety of materials including silicone (PDMS), latex, polyvinyl chloride (PVC), plastic, siliconized latex, silicone elastomers, polytetrafluoroethylene (PTFE), hydrogel-coated latex, and hydrophilic latex coated polymer [10]. The selection of the catheter material is based on the need

of a patient, e.g. for the patients with latex allergies or latex cytotoxicity, the silicone material will be used [11].

*Table 1. 1. Comparison of the advantages and disadvantages of the materials used for urinary catheters.*

<b>Material</b>	<b>Advantages</b>	<b>Disadvantages</b>
<b>Latex</b>	<ul style="list-style-type: none"> <li>• Low price</li> </ul>	<ul style="list-style-type: none"> <li>• inadequate biocompatibility</li> </ul>
<b>Rubber</b>	<ul style="list-style-type: none"> <li>• Simple to process</li> <li>• a strong tensile capacity</li> </ul>	<ul style="list-style-type: none"> <li>• causes latex allergy, which is more common in patients</li> </ul>
<b>Silicone rubber</b>	<ul style="list-style-type: none"> <li>• long period before encrustation and obstruction occurs.</li> <li>• No allergy symptoms</li> <li>• abrasion resistance that is in the middle</li> <li>• Surface lubrication is more effective.</li> <li>• It is biocompatible.</li> <li>• excellent heat and chemically stable (-80 to +230 C)</li> </ul>	<ul style="list-style-type: none"> <li>• Some patients experience discomfort because of its rigidity.</li> </ul>
<b>PTFE coating</b>	<ul style="list-style-type: none"> <li>• Relatively biocompatible; low friction; hydrophobic and self-lubricating</li> </ul>	<ul style="list-style-type: none"> <li>• Toxic, Stiff, and prone to infection and encrustation</li> </ul>
<b>Polyvinyl chloride</b>	<ul style="list-style-type: none"> <li>• Durability</li> <li>• chemically inert</li> <li>• Inexpensive</li> </ul>	<ul style="list-style-type: none"> <li>• Concerns about chemicals that can leak in vivo and cause a few problems</li> </ul>
<b>Polyurethane</b>	<ul style="list-style-type: none"> <li>• outstanding biocompatibility</li> </ul>	<ul style="list-style-type: none"> <li>• Sensitive to heat</li> </ul>

- 
- Excellent tensile strength, but softens in the body
- 

Because of the better non-allergic and smooth flow of urine as well as they retain their shape, so that due to these few properties silicone rubber catheters are preferred over many others. Also, CDC known as the center for disease control and prevention recommends employing the use of silicone material catheters rather than those made up of different materials for patients who experience frequent blockage and to minimize the urinary micro trauma [12]. Antifouling or bactericidal coatings are added/ coated onto the urinary catheter materials to stop the bacterial colonization and biofilm formation as the material the urinary catheters are made of is itself not enough to fight against the pathogens as the bacteria responsible for causing CAUTI are still able to colonize and cause bacterial infections.

### **1.1.3. Methods for Limiting CAUTI with Antibacterial Coatings**

The urinary catheters are improved by adding antibacterial coatings to avoid such microbial colonization and biofilm formation [13]. An ideal antibacterial coating agent should be biocompatible and does not cause any harm to the patient. Also, it should be readily available, inexpensively attached itself to the catheter surface and possess high antibacterial activity. Antibacterial agents target the microbes in a variety of ways, including (1) cell walls inhibition, (2) proteins inhibition, (3) nucleic acids inhibition, (4) targeting cell membrane sterols, and (5) inhibiting specific metabolic steps [14]. Different antibiotics either target components exclusive to each bacterial strain in these groupings or factors that are present in all bacterial species.

Antibiotics and metal ions are the most widely used antimicrobials, but other antimicrobials, such as bacteriophages, natural bioactive compounds, and coatings that are responsive to microbes, are also becoming popular. This section will concentrate on the modification and coating that we have done for the urinary catheter.

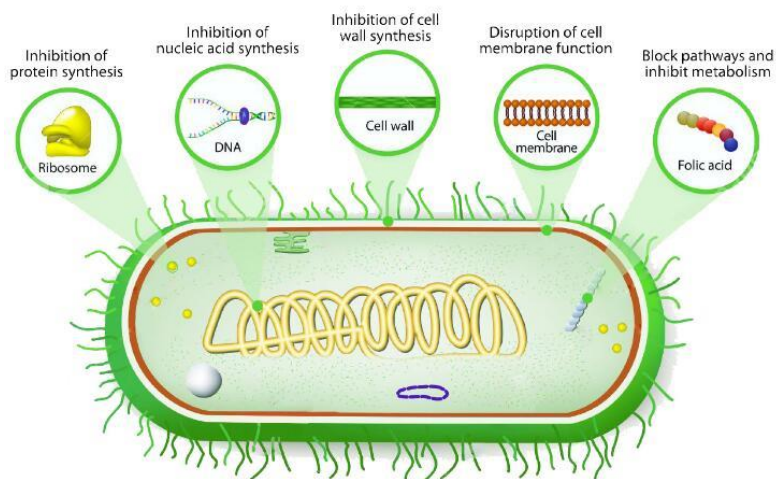


Figure 1. 2. Shows the possible multiple action of inorganic antibacterial agents against pathogenic microbes.

## 1.2. Brief description of this study

Urinary catheter is a medical device whose main function is to drain the urine from bladder, it improves a patient's quality of life. Though the placement of catheter increases the risk of the patient developing a UTI or catheter associated (CAUTI). Silver has gained popularity over the years due to the long-term biocidal properties, high thermal stability, low volatility, also silver coated polymers have gained special attention in recent research because of their antibacterial properties. The toxicity of silver towards mammalian cells is known to be low and does not cause any microbial resistance. Various bacterial strains and micro-organisms can be dealt with using Ag as an antibacterial agent in treating many infections. At nanoscale, silver express notably amazing physiochemical, biological properties, and antibacterial activity. The stable, durable, biocompatible and nontoxic nature of ZnO has drawn more attention in biomedical use. [15]. The size, surface area and ZnO NPs concentration contribute to the bacterial activity. As we know the importance of Ag NPs through different research being done on it, through biotechnological and biomedical perspective. The metal/metal oxide nanoparticle can be stabilized and dispersed by using Graphene based nanocomposites (GBNs) as a nanoscale building block. After hybridization, nanocomposites can typically provide an antibacterial effect that is superior to that of the individual components. In this work we have reported for the first time GO-Ag-ZnO nanocomposite as antimicrobial coating on silicone rubber for urinary catheters. Based on their antibacterial efficacy and potential in biomedical applications, these

materials were selected as antibacterial agents. The results were then extracted through the information on bacterial susceptibility and their action on gram negative and gram positive bacteria.

### **1.3. Objectives**

Against this backdrop a study was undertaken with the aim to prepare an effective antimicrobial coating for urinary catheter, the synthesis of Ag NPS, ZnO NPs and graphene oxide and their binary as well as tertiary nanocomposites. Gram +ve and Gram -ve bacterial strains were tested against the composite for its efficiency. The method applied so far was more convenient and rapid.

- 1) Synthesis of Silver (Ag) NPs, Zinc oxide (ZnO) NPs, Graphene oxide GO.
- 2) Synthesis of Ag-ZnO, GO-ZnO, GO-Ag and GO-Ag-ZnO nanocomposite.
- 3) Investigation of the prepared nanocomposites through various characterization techniques.
- 4) Application of the prepared nanocomposite for the coating of a silicone rubber urinary catheter
- 5) Investigation of the prepared composite and coated films against gram-negative and gram-positive bacteria.

This thesis is divided into six major sections. Chapter 1: The Introduction part, which will give a thorough background relevant to the problem investigated followed by Chapter 2: Literature review, that is related to a brief study done, nanoparticles, and the previous work that has been done. Chapter 3: Experimental section where a detailed experimental procedure will be presented. Chapter 4: Results / discussion, and finally conclusions.

## **Chapter 2**

### **Literature Review**

#### **2.1. Nanotechnology**

##### **2.1.1. Introduction**

Nanotechnology has been defined as research at atomic or macro/molecular level. Nanoparticles are the building blocks of nanotechnology, having at least one dimension less than 100nm. Over the years these nanoparticles in various sizes have been used by several industries and mankind, however, there has been a recent resurgence because of the ability to synthesize and manipulate these particles. These innovative nanoscale particles have been exploited in a variety of different areas such biomedical equipment, medicines, makeup, and green energies. Nanoparticles act as a strong link between bulk materials and atomic/molecular structures. Size, shape, and the physical qualities of the bulk material remain constant. At nanoscale, the morphological features of the substance, aspect ratios, the size and shape are the primary factors of chemical, biological and physical properties. Materials react differently at nanoscale and appear with a few new characteristics including some materials being explosive (e.g., aluminum) or changing their melting point (e.g., gold and silver).

##### **2.1.2. Synthesis of nanoparticles**

At nanoscale, atoms and molecules which are the fundamental units of matter can be precisely manipulated and controlled to produce innovative materials. There are primarily two production methods, bottom-up and top-down approach.

Bottom-up approach is the manipulation of the fundamental components such as atoms or molecules into small structures by using chemical or physical forces. It is the building of material atom by atom, molecule by molecule or cluster by cluster. By using fine force microscope atoms can be pushed into desired locations, even materials can be carved by using a high beam of electrons or heavy metal ions. Examples of bottom-up approach include self-assembly and molecular patterning.



Top-down approach is the breaking of bulk material into nanosized particles and structures. This approach is already being used in synthesizing nanoparticles for various applications. Examples include various lithographic processes for cutting (such as X-ray, electron, or photo ion beam lithography cutting), etching, grinding, and ball milling.

## 2.2. Nanoparticles as antibacterial agents

Nanotechnology plays an important role in treating infectious diseases caused by bacteria and viruses. Antibacterial properties of nanoparticles are widely proven and show significant response even at low concentration due to their higher surface to volume ratio, their physiochemical and biocidal properties. Antibacterial agents are known as the ones possessing antibacterial properties, mainly their function is to inhibit the growth or kill the microbial pathogens namely, bacterial, fungi and viruses. Many types of antibacterial agents including inorganic, organic compounds and carbon-based compounds can be utilized by combining it with other materials to induce antibacterial activity. Combinations are often made by the addition of antibacterial agents as a coating or into the matrices, covering them by the immobilization of composites to achieve antibacterial capability. Most of the inorganic antibacterial agents are made from metal-based elements, whereas most of the manufactured medicines or the naturally occurring materials are the source of organic antibacterial agents.

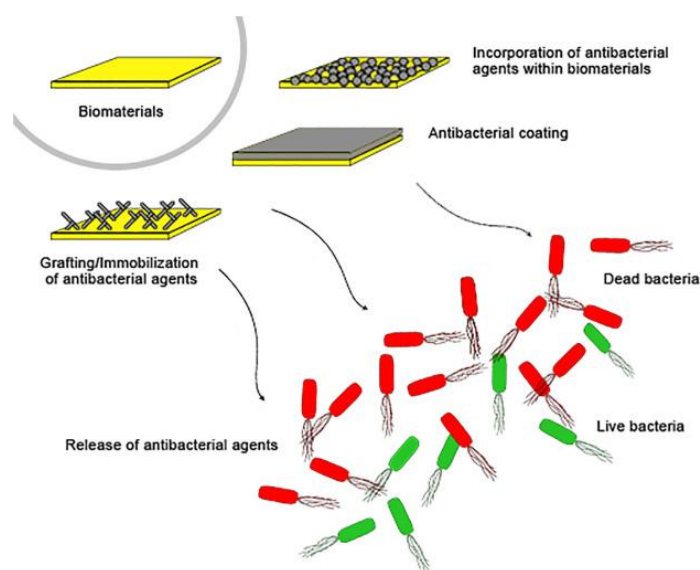


Figure 2. 1. Different methods of combining antibacterial agents with biomaterials

Due to the numerous drawbacks of organic antibacterial agents, that include lower resistance to heat, high decomposability and brief span of life that all adds up to the restriction of these agents in many applications. Antibacterial agents including inorganic compounds have gained popularity in the recent years due to its reduced toxicity, better durability, decreased resistance and excellent selectivity are the reasons why inorganic compounds have more advantages than organic compounds. Ag, Cu, Au, MgO, ZnO, FeO CaO, metal and metal oxide nanoparticles are just a few inorganic compounds that are known to exhibit antibacterial action. Single-walled carbon nanotubes (SWCNT) and graphene oxide (GO) are carbon-based materials which show strong antibacterial activity against many pathogenic microorganisms.

### **2.2.1. Silver nanoparticles**

Silver (Ag) is a conductive, antibacterial agent which is a white shiny transition metal, being used in many industrial and in biomedical applications. Antibacterial action of Ag is primarily caused by the release of ions through a surface containing Ag and these ions interact with the groups attached to enzymes and proteins which support the bacterial life and hence result in destroying the cell wall.

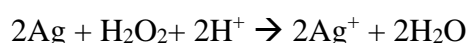
Metallic particles can be considered as nanoparticles when their size is in the range of 1-100nm. Silver is the only transition element that has been synthesized and extensively studied at nanoscale. Owing to their unique properties, Ag NPs have grown in popularity. Silver nanoparticles' size, shape and morphology are influenced by different synthetic approaches, reaction conditions, stabilizers and reducing agents. It can be synthesized through various techniques, commonly used method is the chemical reduction method or by heating or vaporization of a metal in an inert gas /vacuum, which results in the formation of metal atom aggregates.

Various applications of Ag NPs have been found in the different fields of biomedical and medicines. As an example, they can be used in biosensors, in medical devices because of their broad antibacterial activity spectrum and in drug delivery. Ag NPs at low concentration inhibit the growth of bacteria than the antibiotic and as of now no side effects are reported. [16]

### 2.2.1.1. Antibacterial mechanism of Ag NPs

Ag NPs antibacterial mechanism can be explained through various routes whereas the most accurate mode of action is not yet completely clarified. But some possibilities and theories have been approved. Almost all studied silver nanoparticles have strong bactericidal activity. Effectiveness of Ag depend on the size and shape of nanoparticles that has been synthesized [17]. Small sized silver nanoparticles (< 25nm) were demonstrated to have higher bactericidal activity then the larger particles [18].

Silver is present in many oxidation states ( $\text{Ag}^0$ ,  $\text{Ag}^+$ ,  $\text{Ag}^{2+}$ , and  $\text{Ag}^{3+}$ ) these states have been reported to have an inhibitory effect on various pathogenic microbes commonly present in nature [17]. There are number of routes which can define the antibacterial mechanism of Ag NPs [19] where as the most accurate antibacterial action mechanism is unclear. Few of the mechanism routes responsible are based on the penetration of  $\text{Ag}^+$  ions into the cell wall of bacteria, damaging DNA and protein of the bacterial membrane [20] results in the inability of bacterial cells to replicate and results in cell death. Sulfur and phosphorous are the major components of DNA. Therefore, silver nanoparticles have the potential to bind with these groups of protein and destroy DNA. In a study by Danilczuk and coworkers, the generation of reactive ion species on silver nanoparticles was demonstrated. As in a physiological environment the silver ions interact with hydrogen peroxide  $\text{H}_2\text{O}_2$  and generate  $\text{Ag}^+$  ions. Asharani et. al [21] reported an equivalent reaction for silver nanoparticles dissolution.



The reaction mentioned above is happening in mitochondria where there is an abundant amount of hydrogen ( $\text{H}^+$ ) ions. A mechanism was proposed by Choi.et.al. [22] on how Ag NPs dissolves in the presence of oxygen ( $\text{O}_2$ ) ion, reaction is given in the equation below.



Sulfur and phosphorous are the soft basis which make up most of the bacteria and cells and they combine with the soft acids of Ag, causing cell death. Therefore, Ag NPs could react with these soft basis (sulfur and phosphorus ) and destroy DNA [23] [24].

### 2.2.1.2. Comparative studies

The following table shows the previous work related to antibacterial activity of AgNPs as the antibacterial agent, experiment that was applied and the tested microorganism.

Table 2. 1. Comparison of the antibacterial studies performed on AgNPs.

Antibacterial agent	Experiment	Result	Reference
Ag NPs	AgNPs were synthesized by reducing silver nitrate using sodium borohydride.	AgNPs average zones of inhibition for the bacteria E. coli and S. aureus were 7.7 mm and 7.0 mm, respectively.	[25]
Ag NPs	AgNPs with different sizes were synthesized through co precipitation method.	5nm AgNPs against S. aureus, B. subtilis, and E. coli, respectively, have 8.9, 10.6, and 8.3mm.	[26]
Ag NPs	Hydrophilic polymer-coated silver nanoparticles (Ag NPs) have antibacterial action against E. coli.	5 mg/L AgNPs prevented 50% growth of E. coli	[27]
Ag NPs	AgNPs synthesized through chemical reduction method against E. coli and S. aureus	0.24 g/moles of AgNPs, 27mm for S. aureus and 23mm for E. coli,	[28]
Ag NPs	AgNPs as antimicrobial agent, a study against (G-) ) And (G+) bacteria.	Staphylococcus aureus 17 mm has the highest level of sensitivity, followed by Escherichia coli 15 mm	[29]

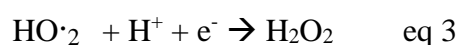
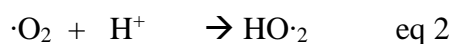
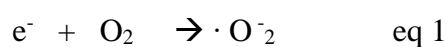
### 2.2.2. Zinc Oxide nanoparticles

ZnO is a powdered inorganic compound which is white in color. ZnO is being used in many fields including everyday applications like in paints, sunscreens, electronics, and pharmaceutical products. It is also being used in industrial sectors and in the field of biomaterials. ZnO exhibits antibacterial property like many other metal oxide groups, and it has been studied at nanoscale range. Because of its small size in nano range <100 nm and larger surface-to-volume ratio. ZnO nanoparticles interact with bacteria more effectively than larger particles do. As a result, nanoparticles have more pronounced antibacterial properties [30]. Recent research has demonstrated that these nanoparticles are selectively harmful to bacteria while having no impact on human cells. The advantage of using zinc oxide as antibacterial agent is that they have some useful mineral elements which are necessary for human beings, and they show excellent bacterial activity at lower concentration, against a wide spectrum of bacteria. Currently, ZnO is registered among the top listed zinc compounds that are considerably recognized as secure, non-toxic materials by FDA the US food and drug administration.

#### 2.2.2.1. Antibacterial mechanism of Zinc Oxide NPs

The accurate toxicity mechanism of ZnO is not clearly demonstrated as it requires a deep explanation, but research have shown that the unique ZnO antibacterial mechanism is due to the interaction of ZnO NPs with the cell wall of bacteria, its core and penetration of these inside the intercellular matrix [31], production of ROS [32] and release of Zn<sup>2+</sup>[33].

One of the most frequently described mechanisms for the metal oxide NPs, responsible for their antibacterial activity is known as ROS production. Superoxide anions (O<sub>2</sub><sup>-</sup>), hydroxyl radicals (HO<sup>-</sup><sub>2</sub>) and hydrogen peroxide (H<sub>2</sub>O<sub>2</sub>) are the main components of ROS mechanism, which cause damage to the cellular components such as DNA, enzymes, and proteins. Generation of these radicals can be explained by these equations. [34]



As mentioned in equation (1) (2)  $O_2$  and  $OH^\cdot$  radicals which are a part of bacterial cell membrane are located on the surface, due to which the penetration of bacteria is not possible into the cell wall as they are negatively charged radical present. Here, the production of  $H_2O_2$  molecules as mentioned in eq (3) are responsible for the cell death of bacteria, as they enter the bacterial cell wall as they have the capability to penetrate.[34]

Another mechanism that is responsible for the bacterial cell death is the release of  $Zn^{2+}$  ions. According to Kasemets et al. [35], ZnO NPs toxicity against bacteria results from ZnO NPs in a solution, which results in the release of  $Zn^{2+}$  ions [36]. Thus, dissolution results in the antibacterial activity of ZnO NPs, the reason is the dissolution of NPs. Li. et. al. [32] reported the release of  $Zn^{2+}$  ions in different mediums used to disperse them. The mediums used were ultra-pure water, sodium chloride, minimal Davis MD, phosphate buffer-saline PBS and Luria-Bertani LB. ZnO NPs at their lower concentration in the medium resulted in less bacterial activity against E. coli. It was concluded that the toxicity of ZnO in different mediums were in the order of Ultra-pure water > NaCl > MD > LB > PBS.

ZnO nanoparticles, on the other hand, having a +ve charge with a +24 mV zeta potential [37]. Due to the electrostatic forces created by the bacteria's and nanoparticles opposing charges, a strong bond forms between the surfaces of the two, causing damage to the cell membrane.

### 2.2.2.2. Comparative studies

The following table shows the previous work done related to antibacterial activity of ZnO NPs as the antibacterial agent, experiment that was applied and the tested microorganism.

Table 2. 2. Comparison of the antibacterial studies performed on ZnO NPs

Antibacterial agent	Experiment	Result	Reference
ZnONPs	Antibacterial activity of ZnONPs was carried out for both gram-negative and gram-positive bacteria	Zone inhibition of ZnONPs against E. coli was $14.17 \pm 0.54$ and against S. aureus it was $11.17 \pm 0.40$	[38]
ZnONPs	The antibacterial efficacy of ZnONPs was investigated against gram-ve (Escherichia coli) and gram+ve (Staphylococcus aureus) bacteria.	At 50 mg/ml concentration of ZnO nanoparticles, E. coli displayed a maximum zone of inhibition $32 \pm 0.20$ , followed by Staphylococcus aureus $24 \pm 0.35$	[39]
ZnONPs	Vancomycin-resistant S. aureus' growth and biofilm formation are inhibited by ZnO nanoparticles	Zone of inhibition for ZnO against S. aureus was 10-36mm and MIC was 0.625 mg/ml	[40]
ZnONPs	In-vitro study of ZnONPs against five bacterial strains	At 2mg/ml the zone inhibition for E. coli and S. aureus are 15 and 17mm, respectively.	[41]



### **2.2.3. Graphene based nanomaterials GBNs.**

Benzene hexatomic ring makeup the main structure of graphene, single layered carbon atoms closely packed in a two-dimensional sheet. [42] Graphene-based nanomaterials (GBNs), including graphene oxide (GO) and reduced graphene oxide (rGO), are readily produced by a variety of surface modifications, and are extensively used in a different fields, including physics, chemistry, biology, medicines [43]. GBNs have demonstrated remarkable potentials in drug delivery [44, 45], sensing/imaging, tissue regeneration [46], and cancer therapy [45, 47], due to their unique features.

Antibacterial capabilities of GBNs have also been used recently [48]. One of the biggest public health concerns is the spread of harmful microbes. The misuse of bactericides and antibiotics led to the gradual emergence of microorganisms with strong resistance to common antibacterial medications, making infection control even more challenging [49]. Antibacterial agents which are antibiotics independent with distinctive mechanisms are of tremendous importance for human health because it is difficult and time-consuming to identify or synthesize novel antibiotics. Gram+ve and gram-ve bacteria are both sensitive to GBNs, as they have emerged as an effective antibacterial agents [50]. The creation of antibiotics that are antibacterial agents with different mechanisms is of tremendous importance and significant for human health because it is difficult and time-consuming to identify or synthesize novel antibiotics. Gram-ve and Gram+ve bacteria are both sensitive to GBNs, which is why they have emerged as effective antibacterial agents. There are numerous derivatives of GBNs, each with unique attributes and capabilities. Here, we focused on GO as antibacterial agent. As we know GO is commonly regarded as the most effective antibacterial nanomaterial among the various GBNs because of its capacity to cut through edges [50, 51], trap cells [52], and reduce oxidative stress. [51]

#### **2.2.3.1. Graphene oxide**

The world's thinnest material is graphene. It is a honeycomb shaped structure made up of a flat layer of  $sp^2$  hybridized carbon that are enclosed in this structure. [53]. Bio scientists have recently become more interested in the 2D flat layer of carbon because of its amazing physiochemical features, and higher biocompatibility [53, 54]. Chemically exfoliated graphite is used to create graphene oxide (GO), which has a few oxygens containing groups such as carboxylic hydroxyl, epoxy, and carbonyl groups. These oxidative functions and the unique nano structure provide graphene oxide

excellent dispersibility in the aqueous media and hydrophilicity, as well as high antibacterial potentials via a variety of processes, which includes the oxidation due to the stress effect, edge, entrapment of the cells and edge cutting effect. GO is a possible candidate for human treatments because of this phenomenon. [55]

### **2.2.3.2. Antibacterial mechanism of Graphene Oxide**

GO is known to have excellent antibacterial properties which can be due to multiple mechanisms. Basically, GO has sharp edges and can physically harm the bacterial cell membranes when they encounter them. As it was reported by Hu et al explained the antibacterial mode of action for GO and the disruption in bacterial cells through TEM [56]. As it was cleared through the TEM and SEM images that when the GO sheets were exposed, the bacterial cell wall was damaged which led to the leakage of intercellular contents. Pham et al reported that the angle at which the sheet contacts the cell membrane, and the edge density are two parameters affecting the antibacterial activity of GBNs [57]. GO sheets have sharp edges and they carry some charge, we all know that the bacterial cell wall is composed of positive and negative charge, so either the antibacterial activity of GO can be due to the charge transfer or the direct cutting affect [50]. Another mechanism which is responsible for the bacterial cell death is the oxidative stress, it causes an imbalance between oxidation and anti-oxidation, which alters bacterial metabolism and cell structure, results in cell death [58]. Another mechanism responsible is cell entrapment, as the bacterial cells are entrapped by the GO sheets when they encounter each other, which results in the isolation of bacterial cells from the external environment thus no access to nutrition. The size of GO sheets is correlated with the entrapment of bacteria. It has been demonstrated that expanding the lateral dimensions of GO improves its antibacterial capabilities [59].

### 2.2.3.3. Comparative studies

The following table shows the previous work related to antibacterial activity of GO as the antibacterial agent, experiment that was applied and the tested microorganism.

Table 2. 3. Comparison of the antibacterial studies against GO

<b>Antibacterial agent</b>	<b>Experiment</b>	<b>Result</b>	<b>Reference</b>
<b>GO</b>	Graphene oxide nanosheets against the G+ and G- bacteria.	For 1mg, the zone of inhibition for E. coli, S. aureus is 19mm and 27mm, respectively.	[60]
<b>GO</b>	Graphene oxide sheets as bactericidal agent for water disinfection	10mm zone of inhibition for E. coli and 9mm for S. aureus.	[61]
<b>GO</b>	Graphene oxide coating onto polymeric substrate	For E. coli and S. aureus, the GO coatings significantly reduced viability by up to 85.8% and 72.4%, respectively.	[62]

### **2.3. Nanomaterials based composites.**

Nanocomposites are the materials made up of nano sized particles which are imbedded into the matrix of a material. Their physical, electrical properties, mechanical strength, toughness, and thermal conductivity all significantly enhance because of the binding of nanoparticles with the material. Due to the efficiency of the nanoparticles, only about 0.5 to 5% of nanoparticles to the total material is typically added. When compared to their bulk sized equivalents, nanoparticles' characteristics are drastically different because of its extraordinarily surface to volume ratio. Additionally, it modifies how the nanoparticles adhere to the bulk substance. The composite can be far better than the component elements as a result. There are some nanocomposite materials that have been demonstrated to be 1000 times more durable than their bulk component components.

Nanocomposites can significantly enhance qualities like

- Optical clarity
- Thermal stability
- Chemical resistance
- Surface modifications
- Mechanical properties
- Electrical conductivity

Due to the characteristics like extraordinary surface area, their ability to provide active sites on the edges and surface of the material for the functional groups, many nanomaterials have recently become more and more popular [1]. However, NPs must be improved to be enhanced to express intriguing new qualities through functionalization of various groups. Currently, a variety of applications including biosensors, medication, devices for energy storage, and electrochemical devices, make extensive use of carbon-based materials. The excellent functionalization and chemically exfoliated graphene oxide (GO) with oxidative groups such as epoxide, hydroxyl, carboxylic, and the carbonyl group are considered cost effective and high dispersion nanomaterials for various applications. The metal/metal oxide nanoparticle can be dispersed and stabilized using graphene-based nanocomposites as a nanoscale building block [63]. After hybridization, nanocomposites can typically provide an antibacterial effect that is superior to that of the individual components. As we know,

Ag ions are released from its surface, Ag NPs have excellent antibacterial potential against different pathogens. By damaging the bacterial cell membrane and DNA replication [64], they cause their cell death. Sadly, the spontaneous aggregation of Ag NPs greatly restricts their useful uses. GO appears to be a reliable carrier at this stage for dispersing Ag NPs and enhancing their antibacterial properties. According to reports, GO and Ag NPs nanocomposites have increased antibacterial activity [65], Ag NPs adsorbed on graphene oxide hinders the aggregation of GO sheets because it can prevent the nucleation of Ag NPs. The stability of Ag NPs and GO was increased by the formation of a nanocomposite, leading to an increase in effectiveness. In a study by Zhu et al. claimed if the concentration of cations on the surface of the composite is higher [66], it improves the contact of bacterial cell membrane with the composite, and is also responsible for the improved antibacterial impact of GO-Ag NPs nanocomposites [67].

The oxides of the metals have also frequently been employed to create nanocomposites with GBNs. One of the common examples is the nanocomposite of GO and ZnO. According to reports, the GO-ZnO nanocomposite's antibacterial activity is correlated with cellular membrane stress caused by sharp edges [68]. Another significant element is the concentration of ZnO affecting the antibacterial performance of GO-ZnO nanocomposite. By increasing the ZnO concentration the antibacterial activity of ZnO on *E. coli* was improved because of increased osmotic pressure, it causes the bacteria to lose their viability [69].

Since the development of nanotechnology, several human and animal infections can be controlled by using Ag and ZnO nanocomposite, which has improved antibacterial activity on a nanoscale. Ag-ZnO nanocomposite is being widely used in many fields [70]. Because of their excellent thermal conductivity, stability, and antioxidant capabilities, they are widely used by researchers in biosensors and as antibacterial agents in biological research.

### 2.3.1. Comparative studies

The following table shows the previous work related to antibacterial activity of GO as the antibacterial agent, experiment that was applied and the tested microorganism.

Table 2. 4. Comparison of the antibacterial studies performed on GBN based nanocomposites.

<b>Antibacterial agents</b>	<b>Experiment</b>	<b>Result</b>	<b>Reference</b>
<b>GO-Ag NC</b>	Fabrication of GO-Ag nanocomposite with different AgNPs to GO ratio.	GO-Ag NC was more toxic to E. coli than S. aureus.	[71]
<b>GO-Ag NC</b>	Antibacterial activity of the prepared GO-Ag NC	ZOI for E. coli 18mm and S. aureus 17mm.	[72]
<b>GO-Ag NC</b>	GO-Ag NC was used to combat methicillin-resistant Staphylococcus aureus.	The results showed antibacterial activity against S. aureus	[66]
<b>GO-ZnO NC</b>	Prevention of wound causing infections by using GO-ZnO NC	GO-ZnO NC (0.3M) conc. exhibit higher efficacy against bacterial strains	[73]
<b>Ag-ZnO NC</b>	Ag-ZnO nanocomposite as an antibacterial agent against the anaerobic oral pathogen	Ag-ZnO NC showed great antibacterial activity as compared to ZnO.	[74]
<b>GO-Ag NC</b>	Synthesis of GO-Ag as bactericidal agent for wastewater treatment	S. aureus was reduced by 87.6%, and E. coli by 100%.	[61]

# Chapter 3

## Methodology

### 2.4. Chemicals and Materials

Zinc acetate dihydrate ( $ZnC_4H_6O_4$ ), Sodium hydroxide (NaOH), Silver nitrate ( $AgNO_3$ ), Sulfuric acid ( $H_2SO_4$ ) 98%, Graphite flakes were procured from Sigma Aldrich, Germany. Distilled water, hydrophilic PTFE 0.2  $\mu m$ , 47mm were used for filtration purposes. RCI Labscan provided absolute ethanol (40%) for the experiment. Merck provided potassium permanganate ( $KmNO_4$ ) and  $H_3PO_4$  (85%). Dae-Jung Chemicals and Metals Co. Ltd provided the sodium borohydride ( $NaBH_4$ ) and hydrazine ( $N_2H_4.H_2O$ ) (98%) used in the experiment. Silicone sheet 1MM was procured through scientific hub (pvt). ltd. The materials were used without further purification or treatment; they were received in that state.

### 2.5. Ag NPs synthesis

Ag NPs were created through a chemical reduction process. Briefly, 40ml DI water, 30mg of  $AgNO_3$ , and 60ml (0.05M, 270mg) of  $CH_3COONa$  solution were added to a volumetric flask. The mixture was created uniformly. Add 20 $\mu l$  of the reducing agent  $N_2H_4$  to this mixture. After adding  $N_2H_4.H_2O$ , the solution instantly became black, signifying that the  $Ag^+$  ions had been reduced. After 3 hours of room temperature stirring a translucent solution was formed. [75]. The solution obtained was filtered and centrifuged by using DI water as a solvent. Dried at 80°C, shiny silver nanoparticles were obtained.



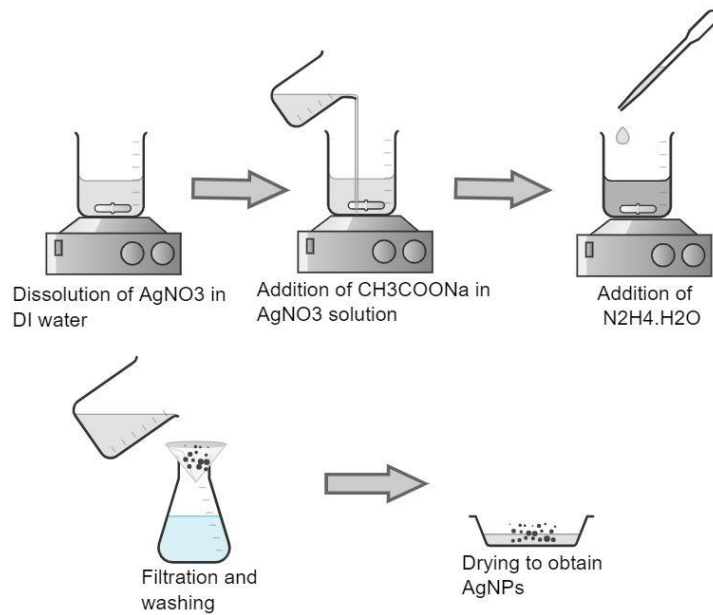
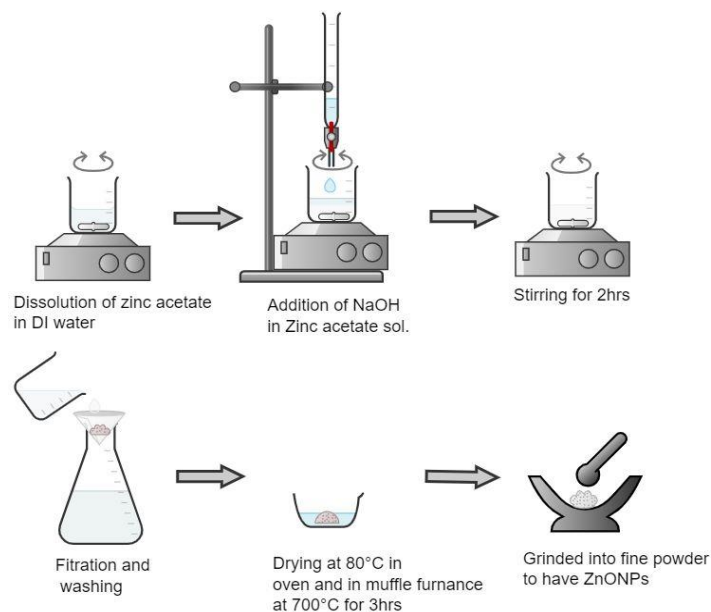


Figure 3. 1. Synthesis of AgNPs

## 2.6. ZnO NPs synthesis

A chemical reduction method was used for the synthesis of ZnO NPs. Zinc acetate 1M was added to 20ml DI water and kept stirring for 2hours. Drop by drop addition of 2M solution of sodium hydroxide (1d/se) into the zinc acetate solution. The obtained solution was kept at stirring for 2hours. It was allowed to settle overnight. Then wash and filter by using DI water few times. Overnight drying at 80°C. Kept at 700°C in muffle furnace for 3hours. It was grinded into fine powder by using mortar pestle. [76]



## 2.7. In-situ synthesis of nanocomposite

Ag-ZnO nanocomposite was prepared through the in-situ method. 1g ZnO and 0.105g of NaBH<sub>4</sub> was mixed in 50ml of DI water under stirring with the addition of silver nitrate 2M. Stirring was done at 60°C for 1 hour, the solution was filtered with DI water several times. Greyish black colored Ag-ZnO powder was obtained after drying at 60°C for 1hour.

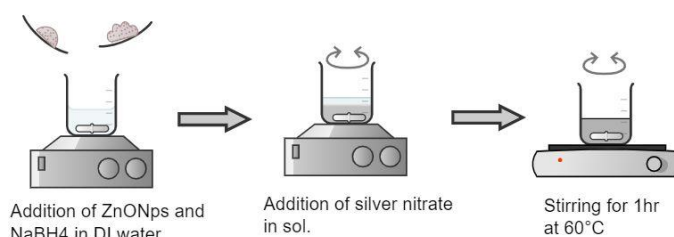


Figure 3. 2. Synthesis of ZnO NPs

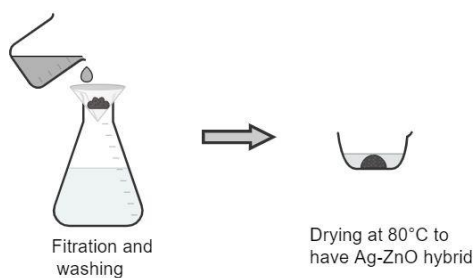


Figure 3. 3. Synthesis of Ag-ZnO nanocomposite

## 2.8. Graphene oxide GO and its nanocomposites synthesis

GO was first prepared alone and then later it was combined with Ag NPs, ZnO NPs and Ag-ZnO nanocomposite to form GO nanocomposite. All these reactions were conducted separately to obtain separate hybrid composites along with Graphene oxide.

## 2.9. Graphene oxide synthesis

Improved hummers method was used to prepare graphene oxide [77]. 360ml of sulfuric acid and 40ml of phosphoric acid were added into a beaker and stirred for 30minutes on an ice bath. 3g of graphite powder was added and stirred for 10mins. Now add 18g of potassium permanganate into the solution and stir it for 30 minutes. From purple color the solution turns to muddy green. After that, the ice bath beneath the reaction container was removed and stirring was done for 16hrs at 50°C. The solution turns dark brown after 16hr stirring, add DI water 100ml very slowly (exothermic reaction) into the solution. H<sub>2</sub>O<sub>2</sub> 10ml was added dropwise into the KMnO<sub>4</sub> solution to stop the reaction. The change in color indicated GO formation and its oxidation, as it changes to bright yellow. DI water and ethanol were used for the washing of GO. Finally, the product was centrifuged at 4000 rpm until the pH 7 is achieved. The solid obtained after centrifugation was kept at 60°C in a vacuum oven for overnight drying.

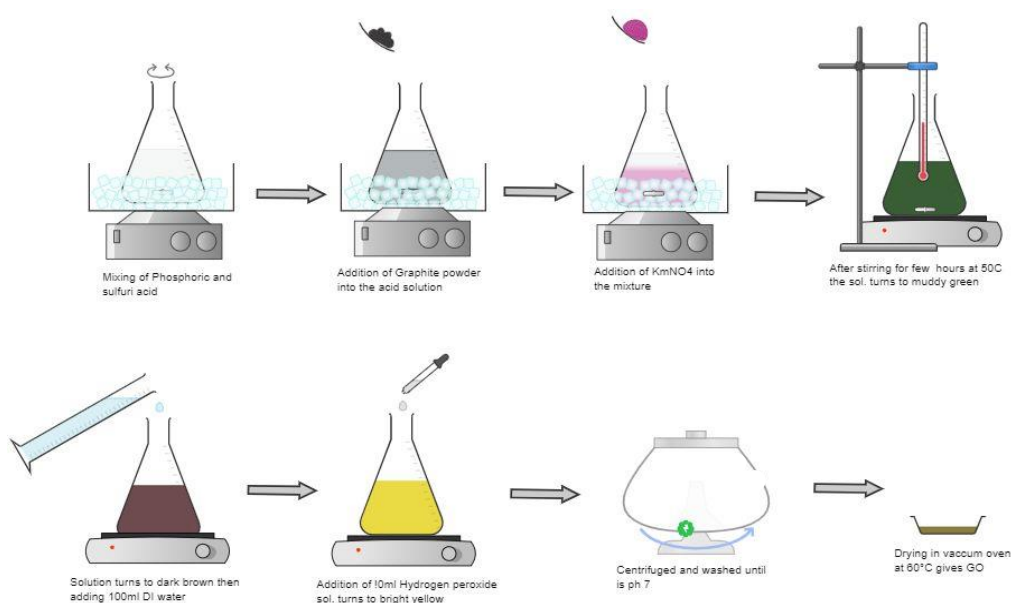


Figure 3. 4. Synthesis of Graphene oxide

## 2.10. GO-Ag, GO-ZnO, GO-Ag-ZnO nanocomposite synthesis through in-situ method:

### 2.10.1. GO-ZnO synthesis.

GO-ZnO nanocomposite was prepared through In-situ method [78]. In 40ml of DI water 0.1g of already prepared GO was dispersed by ultra sonication for 1hr. In this GO suspension zinc chloride (1.0mmol) and sodium hydroxide (10.0mmol) were dissolved. Stir at 90°C for 6hrs. Centrifugation of the mixture was done at 4000 rpm to remove the supernatants and the remaining residue was cleaned 5-6 times using DI water and ethanol. The solid sample obtained was dried for three hours at 80°C.

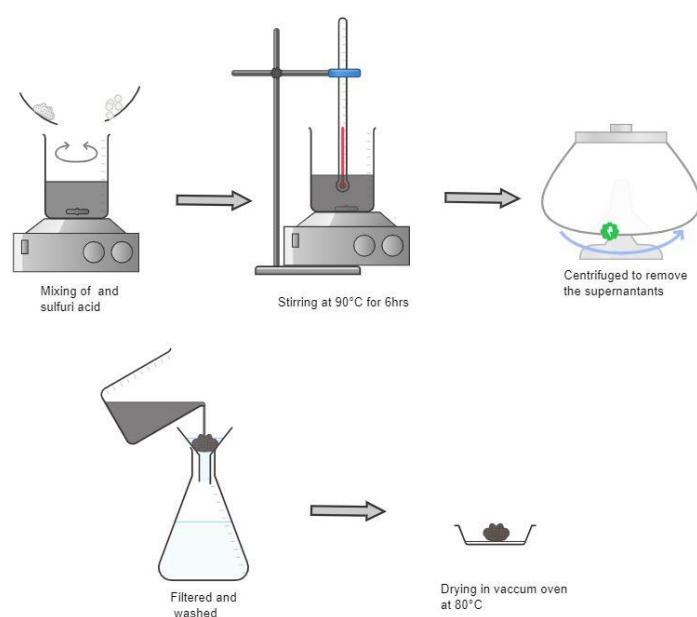


Figure 3. 5. Synthesis of GO-ZnO nanocomposite

### 2.10.2. Synthesis of GO-Ag

GO-Ag nanocomposite synthesis was done by adding 5mg GO to 1ml DI water and sonicated for 30mins. After that  $\text{AgNO}_3$  4mM in 2ml DI water was added to GO suspension along with the addition of sodium citrate solution 10mM in 1ml DI water. Stirring was done for 30mins. Afterwards drop wise (1d/s) addition of sodium borohydride solution 10mM in 1ml, further stirred for 5hr's [79]. A greenish brown color was obtained which was centrifuged at 4000 rpm 4-5 times. Ethanol and DI water were used for the washing of the obtained solid. Vacuum drying was done overnight at 60°C.

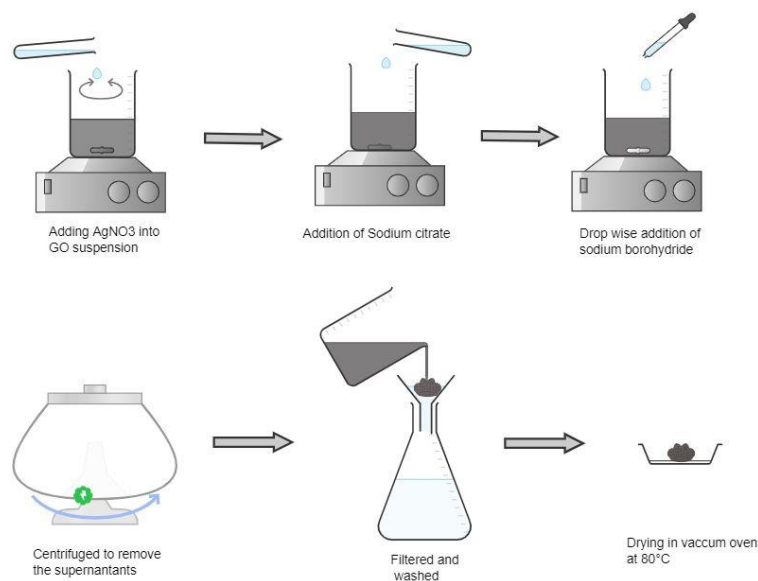


Figure 3. 6. Synthesis of GO-Ag nanocomposite

### 2.10.3. GO-Ag-ZnO nanocomposite synthesis

GO-Ag-ZnO nanocomposite was prepared by In-situ method as reported in this report [80]. Firstly, ZnO nanoparticles were prepared by the drop wise addition (5ml/min) of 25ml of NaOH 0.4mol/l into 0.2mol/l ZnSO<sub>4</sub> in 20ml solution. Stirring of the mixture was done for 60min. Then the solution was kept for 2hours at 60°C under stirring. Ascorbic acid 0.01mol/l in 60ml DI water was added to the above mixture as reducing agent. Now in NaOH, ZnSO<sub>4</sub> solution 13ml of silver nitrate 0.01ml was added. Stirring was done for 2hrs at 70°C. 50mg of previously prepared GO was added into 50ml DI water, it was sonicated for 30 minutes. GO suspension was added to the above solution prepared. Stirring was done for 2hrs at 70°C. Final obtained solution was centrifuged, washing was done by using DI water. At 70°C the sample was dried in a vacuum oven for 24hr.

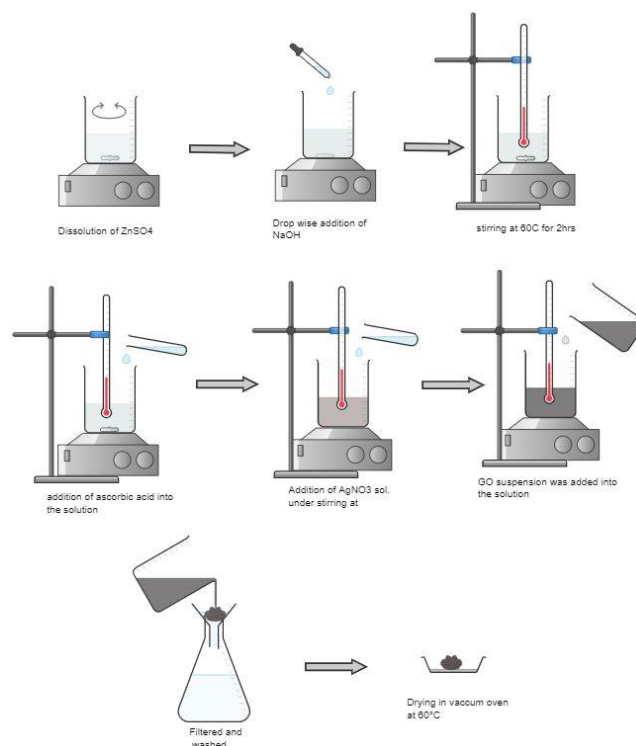


Figure 3. 7. Synthesis of GO-Ag-ZnO nanocomposite

## 2.11. Thin film preparation onto silicone rubber

For the deposition of thin films of Ag NPs and GO-Ag-ZnO nanocomposite, silicone rubber was used as a substrate.

### 2.11.1. Cleaning of Silicone rubber

Silicone rubber of 2x1 dimension were cleaned by ultrasonication in D.I water, followed by ethanol and DI water for 15 minutes each. They were dried for 30 minutes in a at 37°C. Then the substrate was subjected to plasma cleaning. Silicone rubber films were then exposed to plasma treatment for 20 mins on each side for further investigations.

### 2.11.2. Deposition of thin film via In-situ synthesis for Ag NPs

Silver nanoparticles were loaded by the in-situ synthesis method [81]. Via ion interchange, Ag ions were immobilized using an AgNO<sub>3</sub> solution. Plasma treated silicone rubber films 2x1 were deposited into the AgNO<sub>3</sub> solution for 1hr, by the addition of sodium borohydride solution and sodium citrate was used as reducing agent to generate silver particles. The immersed thin films changed their color after 2hrs

dipping, which shows the deposition of Ag NPs. A dramatic color change was shown by the thin films when they were immersed in the solution for 2hrs. The silicone rubber films were then dried for 30 min at 37°C to evaporate the solvent and remove the organic residuals.

### **2.11.3. Deposition of thin film via spin coating for GO-ZnO-Ag**

The spin coated technique was used for the coating of GO-Ag-ZnO nanocomposite onto a silicone rubber. For this purpose, 5mg of GO-Ag-ZnO powder was dissolved in 1% polyvinyl alcohol (PVA) which was used as a binder. After a few hours stirring a homogenous solution was obtained. Then the pre plasma treated silicone substrates were coated with nanocomposite. This process was carried out at 2500 rpm for 25s at RT. Then the composite deposited films were washed with DI water gently, dried at 37°C for about 30 min.

## **2.12. Characterization techniques**

### **2.13. X-ray Diffraction (XRD)**

STOE-Germany manufactured a technique known as X-ray diffraction. It is used to investigate the crystallite nature of materials. The crystalline properties of materials serve as a 3-D diffraction grating for x-ray wavelengths comparable to the interplanar spacing in a crystal lattice, according to a 1912 discovery by German scientist Max von Laue and Co.

XRD is used for the identification of crystallite phases and structures in the material. It is used for the determination of film thickness, unit cell dimension, average size, sample purity, also for the microstructure analysis of polycrystalline and amorphous materials.

#### **2.13.1. Working Principle of XRD**

X-ray diffraction is a non-destructive technique used for the characterization of materials using x-ray radiation. XRD analysis is based on the interference between monochromatic X-rays and the specimens that is constructive. Monochromatic radiation is filtered through cathode ray tubes to produce X-rays. Collimation is employed to concentrate these rays before they are focused on the specimen. If the conditions are right, constructive interference will emerge from the interaction of these rays with the specimen. The electromagnetic radiation's wavelength is correlated with

the specimen's diffraction angle and by Bragg's Law. Mathematically it is expressed as,

$$n\lambda=2d_{hkl} \times \sin \theta_{hkl}$$

It is a technique that provides fingerprint of Bragg's reflection in a reciprocal space. These x-rays are produced by bombarding a metal surface, typically Cu with electrons which are then dispersed by an electron cloud that surrounds each atom in the sample. A constructive interface is created when these rays hit the surface and the path  $\lambda = 2d \sin \theta$ , where  $2\theta$  is measured through experiment. As the detector or the sample is moved the crystal acts as a 3D diffraction grating and the maxima of this 3D array can be studied. Each crystal produces a diffraction pattern that is inversely related to the size of crystallite and its crystal plane. Diffraction spots are related to the reciprocal space whereas crystal planes with real space and form a 3D reciprocal lattice.

## **2.14. Scanning Electron Microscope (SEM)**

The morphology of the synthesized nanocomposite was subjected to SEM analysis (JSM-64900). A thin conductive layer of gold was used to cover the samples before the analysis. The surface topography and chemical composition is revealed in the image created by the electrons when they interact with the samples surface.

### **2.14.1. Working principle of SEM**

SEM is an outstanding technique that gives information about the surface of material, crystalline structure, orientation, and the chemical composition of a material. It uses an electron beam to generate the image of the material and the magnifications are obtained by the means of electromagnetic fields. Its resolution is up to one million times to the original size of the object and is used by researchers worldwide to get the resolution to micro and nano level. The resolution of SEM is up to 1000x times of human eye which is 200  $\mu\text{m}$  and that is 0.2  $\mu\text{m}$ . This means that if two objects or features of a material are less than 0.2  $\mu\text{m}$ , then this microscope would not be able to distinguish between the two. The superior resolution as compared to a light microscope is because it utilizes a beam of electrons that are accelerated with a voltage of 100kV. The materials that can be resolved by SEM can be both conductive and nonconductive.



If an EDS detector is attached to the setup, then the elemental analysis of the material can also be done. It can give both quantitative and qualitative information about the material. The samples are placed on a stub in the sample chamber and are typically sputtered with gold to get better imaging.

## **2.15. Fourier Transform Infrared (FT-IR) spectroscopy**

FT-IR spectroscopy is the most widely used vibrational spectroscopic technique for identifying the functional groups or the types of bonds present on the surface. It is the type of spectroscopy in which the infra-red spectrum is studied in the range of whole wavenumbers through the Fourier transform method.

### **2.15.1. Working Principle of FT-IR**

The working principle of FTIR analysis is the light absorbed by the molecules when it falls in the infra-red region. The light absorption corresponds to the bonds present in the molecules. The absorption frequencies were in the range of  $4000-500\text{cm}^{-1}$ . Infra-red absorption spectrum is based on the vibrations of molecules. When the specimen is exposed to these radiations, its molecules absorb radiations of certain wavelength. This changes the dipole movement of specimen molecules. As a result, the energy level of the specimen molecule is transferred to an excited state from the ground state, energy gap between these molecules determines the frequency of absorption peak. The change in intensity is subjected to the dipole moments and shift of energy levels. These energy levels are recorded in the form of peaks and are found in  $4500-1300\text{ cm}^{-1}$  range. Single bonded atoms stretching is found around  $4000-2500\text{ cm}^{-1}$  and if there is hydrogen bonding that is found in this region then the broadening of peaks will be observed. Triple bonded atoms show these frequencies from  $2700-1800\text{ cm}^{-1}$  region. Double bonded atoms range from  $1950-1450\text{ cm}^{-1}$ . The frequency region below  $1300\text{ cm}^{-1}$  is known as the fingerprint region as bands in this region are comprised of sharp peaks that are associated with individual compounds. The working of this spectrometer starts with the IR rays emitted from a source and then directed by an interferometer, that contains moveable and immovable mirrors which partially reflect and focus IR radiation on the sample and then collect them to refocus on the detector. The obtained frequencies are then Fourier transformed by a computer algorithm that is displayed in the form of a graph.

## 2.16. UV-Vis Spectroscopy

This technique involves measurement of light absorption as a function of wavelength that gives information about transition of electrons in the material. It is a method of figuring out the band gap as electrons transition between the conductance and valence shell. It is based on this equation by Bohr-Einstein:

$$\Delta E = E_2 - E_1 = h\nu$$

$\nu$  is the frequency of electromagnetic radiation, links with the molecular or discrete energy states. Here  $h$  is a Planck's constant which is  $6.626 \times 10^{-34}$  Js. Now for optical spectroscopy it is better to use wavenumber  $\tilde{\nu}$  instead of frequency  $\nu$  and the following equation transforms into:

$$\Delta E = E_2 - E_1 = hc\tilde{\nu}$$

The radiations which are absorbed or emitted of having different frequency or wavelength can then be assigned to the difference in energy states. Nowadays the spectrophotometer consists of a visible and UV source that is split up into its constituents by a prism or grating monochromator. This is also called the dispersive method. In a double beam instrument, the beam is split into two paths, one of which contains the reference and the other containing the sample and after this light is refocused and falls on the detector that which generates an AC signal which is then displayed in the form of a wave. Usually, solid particles are dispersed into a solvent to form dispersions and liquids are used as such by varying dilutions. Cuvettes are used for the purpose of measurement and are kept 10-15cm apart

## 2.17. Microbial culture

The cultured microorganisms Gram -ve bacteria *E. coli* and Gram +ve bacteria *S. aureus* were used for the antibacterial studies of the synthesized samples. They were inoculated in Luria-bertain broth (LB) and incubated at 37°C in 100rpm overnight.

## 2.18. Antibacterial activity measurement

The standard disk diffusion method was used for the antibacterial testing of the prepared nanoparticles. Gram-ve *Escherichia coli* and gram+ve *Staphylococcus aureus*, bacterial strains were used for this purpose. The bacterial strains freshly cultured were dropped in an Eppendorf containing broth/PBS solution, then it was shake on a rotatory shaker for about few minutes. Nutrient agar a used to prepare the

agar media used for the growth of bacteria. It was prepared by dissolving 30.5 g of nutrient agar in 800ml distilled water. Prepared agar solution was uniformly poured into petri dishes and was left for few minutes till it solidified and left in the incubator to check for any contamination. Then the cultured bacteria were spread on these plates by using a cotton swab. Different concentrations (2 mg/ml, 1 mg/ml, 0.5 mg/ml) of the synthesized particles Ag, GO, ZnO, Ag-ZnO, GO-Ag, GO-ZnO, GO-Ag-ZnO were subjected to antibacterial assay. Filter paper was cut into 6mm disks, they were dipped in the dilutions for few minutes, the filter papers were then placed over the plates with agar. The prepared petri dishes were then incubated at 37°C for 24hours. After 24hours the plates were taken out and zone inhibition were measured by measuring scale. Before use, all the apparatus including Pipette, petri dishes, media bottle, spreader, forceps, broth, and agar media were autoclaved. Autoclave was used in almost every step to avoid contamination.

### **2.19. Optical imaging**

An appropriate thickness of oxide layers considerably improves the reflectivity contrast of molecularly thin films produced on silicon wafers. A thickness resolution far below 1 nm can be achieved by using this interference enhancement to observe and quantify film topologies. It operates under environmental conditions, is quick, causes almost no sample disturbance, and is cost effective.

### **2.20. Contact angle measurement.**

The wettability of the polymer membrane surface is determined by a factor known as contact angle. In both pure and practical research, it is crucial to determine the interfacial tension between solid vapor and solid liquid. To determine the different attributes of thin film, to study surface energy and the liquid's affinity for the solid surface, contact angle measurement is a simple and efficient method. The thin film efficacy, fouling nature, flux rate, and self-life are all significantly influenced by the thin films wettability or hydrophilicity.

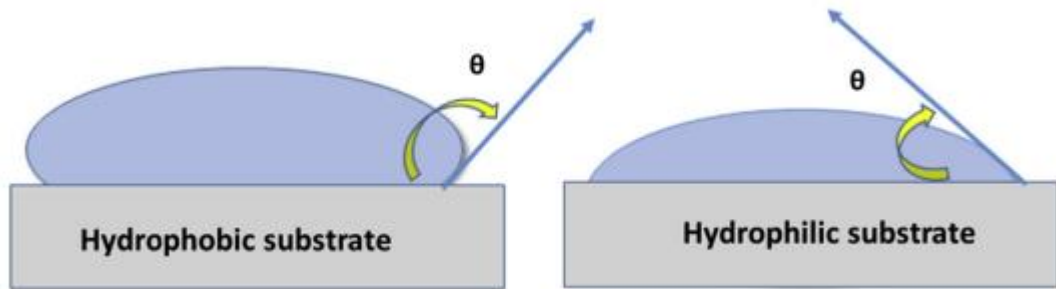


Figure 3. 8. Contact angle measurement.

### 2.21. Plasma treatment

Plasma treatment is a popular technique being used in biomedical field to modify the biomaterials for their safe use in a different field, to enhance their bonding characteristics. Plasma treatment is the conversion of a surface containing low energy to higher energy by removing the hydrogen atoms and replacing them by oxygen containing species, to improve the adhesion to the surface and the removal of contamination. The type of functionalization can be changed by choosing a different plasma gas and operating conditions when using radiofrequency (RF) plasmas (pressure, gas flow rate, power, and time).

# Chapter 4

## Results and Discussion

### 3.1. Instrumentation and measurements

The morphological studies of the samples were investigated through SEM using JEOL JSM-6490A (Tokyo, Japan) with a combination EDAX EDS probe for elemental analysis. The structural information was analyzed by X-ray diffraction (XRD) on Seimens D5005 STOE & Cie GmbH (Darmstadt, Germany) at an angle ( $2\theta$ ) in the range of  $10^\circ$  to  $80^\circ$ . The FTIR analysis was investigated on PerkinElmer, SpectrumTM100 spectrophotometer using potassium bromide pellets with dried powder samples. UV-Vis spectrum was observed via UV-Vis spectrophotometer by OPTIMA (SP-3000DB). The solutions were made in DI water.

### 3.2. Scanning Electron Microscopy (SEM)

The scanning electron microscopy (SEM) was used to analyze the morphological aspects of the prepared/ synthesized samples of Ag NPs, ZnO NPs, Graphene oxide, Ag-ZnO, GO-Ag, GO-ZnO, GO-Ag-ZnO nanocomposites. As shown in the **Figure 4.1 (a)** which shows a relatively uniform distribution of Ag NPs spherical in shape, having an average size of 28nm. **Figure 4.1 (b)** shows the synthesized ZnO NPs of relatively uniform size having an average size of <60nm. SEM images of GO shows the 3D stacked layers of GO sheet as shown in **Figure 4.1 (c)**. In GO-Ag nanocomposite small Ag NPs are decorated onto GO sheets. Ag NPs are randomly distributed on the GO surface having an irregular shape. For GO-ZnO nanocomposite, the visibility of ZnO NPs can be observed as high density of nanoparticles are deposited onto the surface of graphene oxide sheets. For the prepared Ag-ZnO it showed that both products exhibit spherical as well as hexagonal morphology within the structure which confirms the formation of nanocomposite **Figure 4.1 (d) to (f)**. For GO-Ag-ZnO nanocomposite **Figure 4.1 (g)**, Ag-ZnO nanoparticles are homogeneously distributed onto the surface of the GO sheets, which clearly indicates the formation of GO-Ag-ZnO nanocomposite **Figure 4.2 (a) (b)** shows the SEM images of silicone rubber coated with the nano sized Ag NPs with an average size of 43nm.

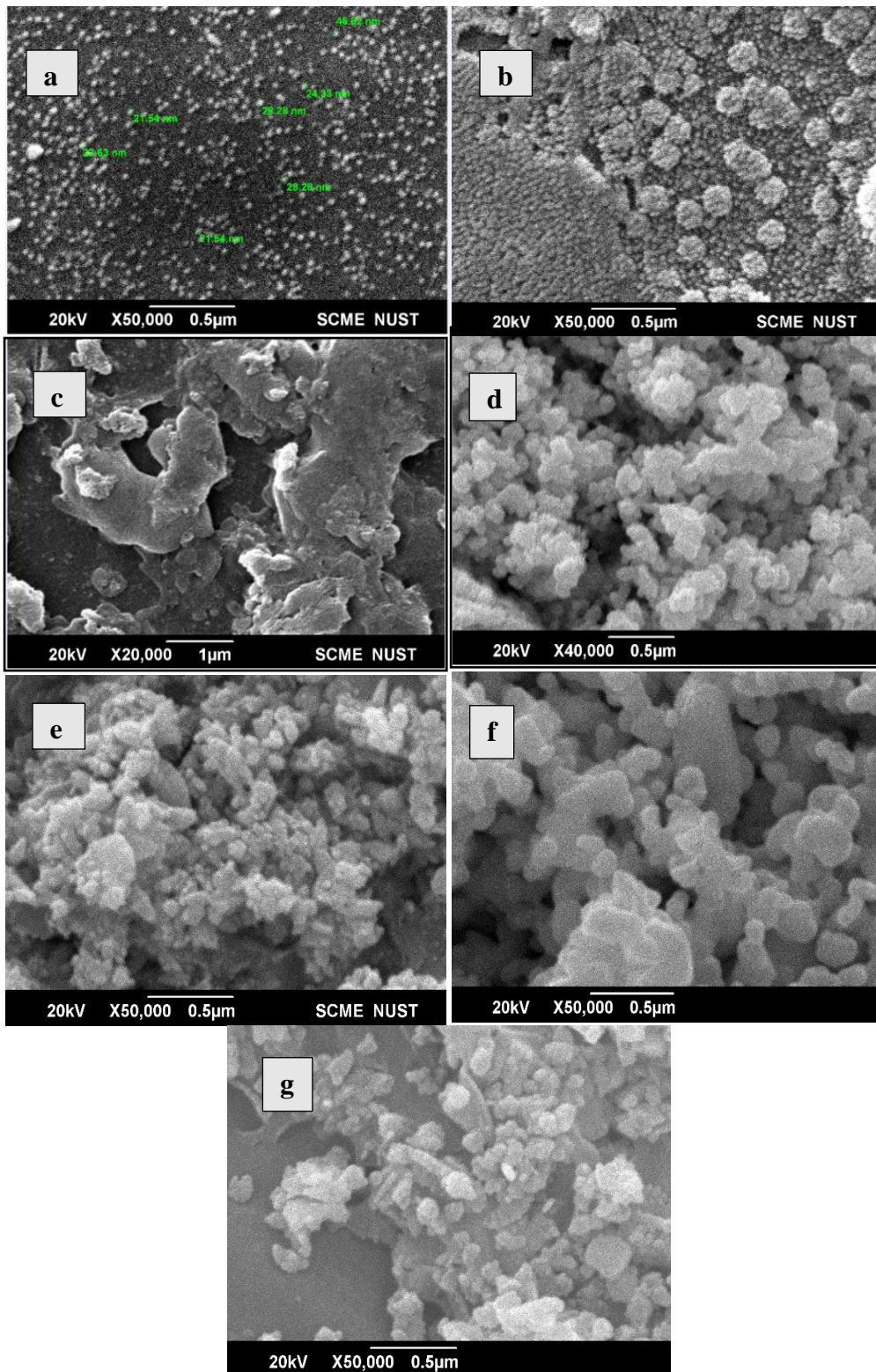


Figure 4. 1. SEM images of a) silver nanoparticles b) Zinc oxide nanoparticles c) Graphene oxide d) Ag-ZnO e) GO-Ag f) GO-ZnO g) GO-Ag-ZnO nanocomposite.

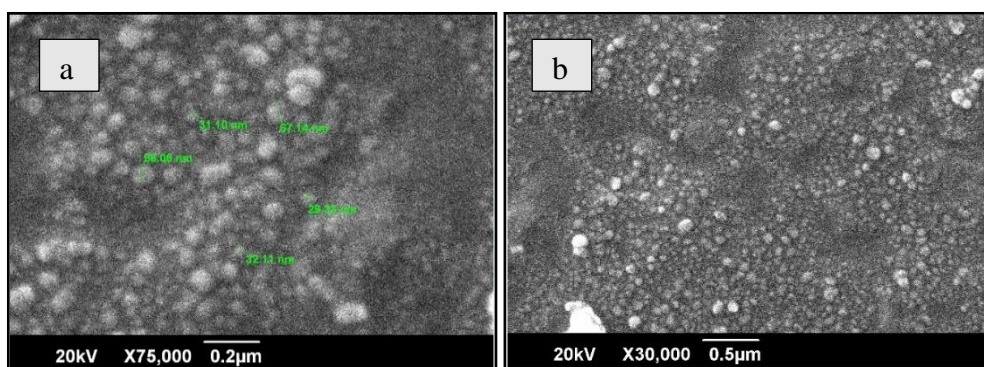


Figure 4. 2. Shows the SEM images of AgNPs coated silicone rubber at higher resolution

### 3.3. Energy-dispersive X-ray spectroscopy (EDS)

The elemental analysis of the synthesized Ag NPs, ZnO NPs and GO along with its composites was done to find out the exact stoichiometric ratios of the elements present. EDS was used to examine the ratio of synthesized materials. The results of the spectrum obtained from the sample can be seen in the figures. The EDS spectrum in **Figure 4.3** shows the higher value of Ag (66.2%) the elemental analysis of Ag shows the spectrum consists of signal from O atoms. It might be due to the X-ray emission from biomolecules responsible for stabilization of nanoparticles. It can be shown in **Figure 4.4** that a significant amount of Zn and O to be present in the sample having an atomic percentage of 1:1. **Figure 4.5** The stoichiometric ratio of GO comes out to be 1:1, shows an amount of 52.5% carbon and 47.5% of oxygen present which indicate the formation of GO.

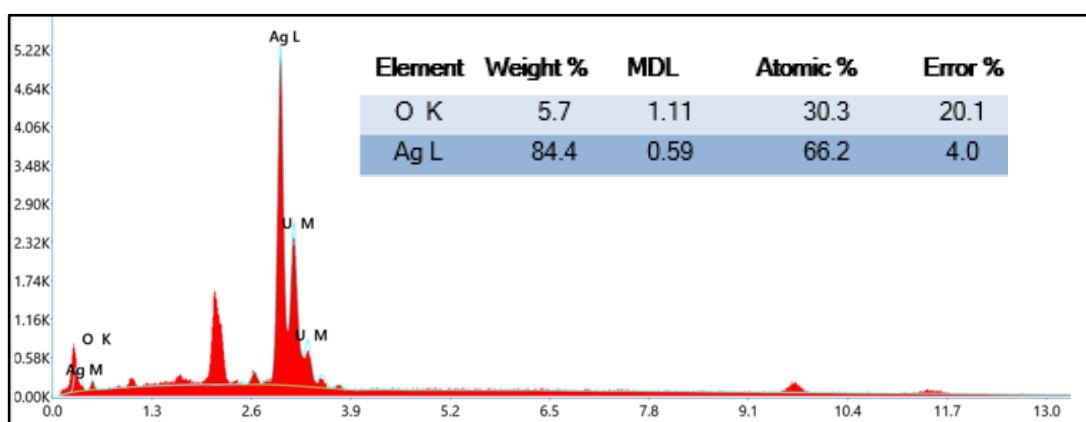


Figure 4. 3. EDS of silver nanoparticles



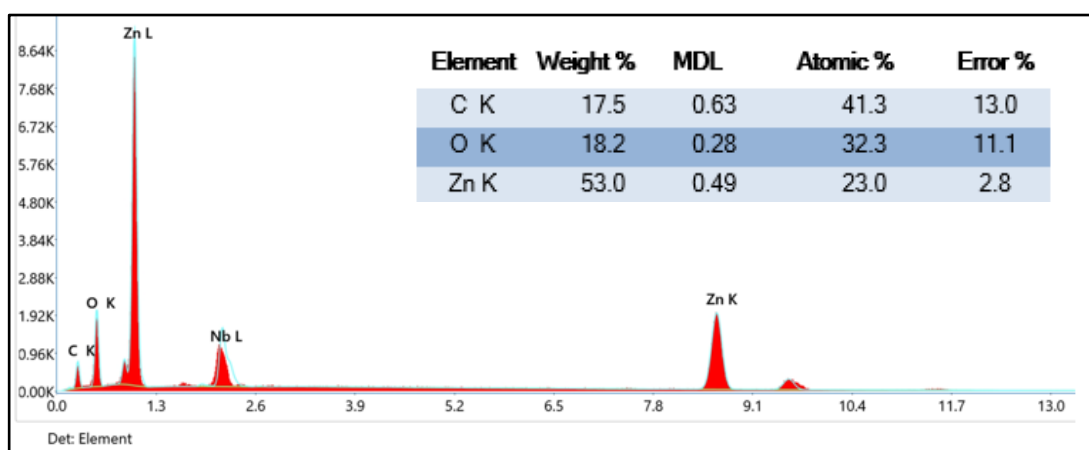


Figure 4. 6. EDS of zinc oxide nanoparticles ZnO NPs

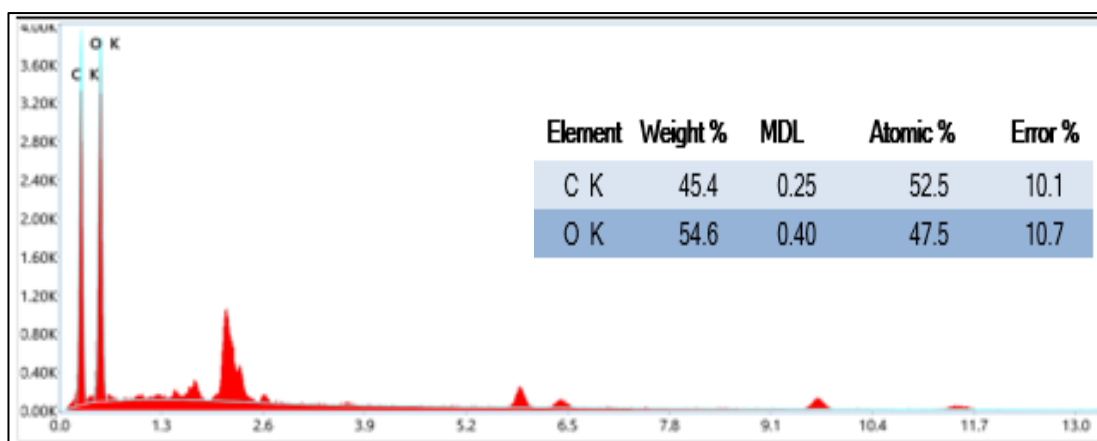


Figure 4. 4. EDS of graphene oxide GO

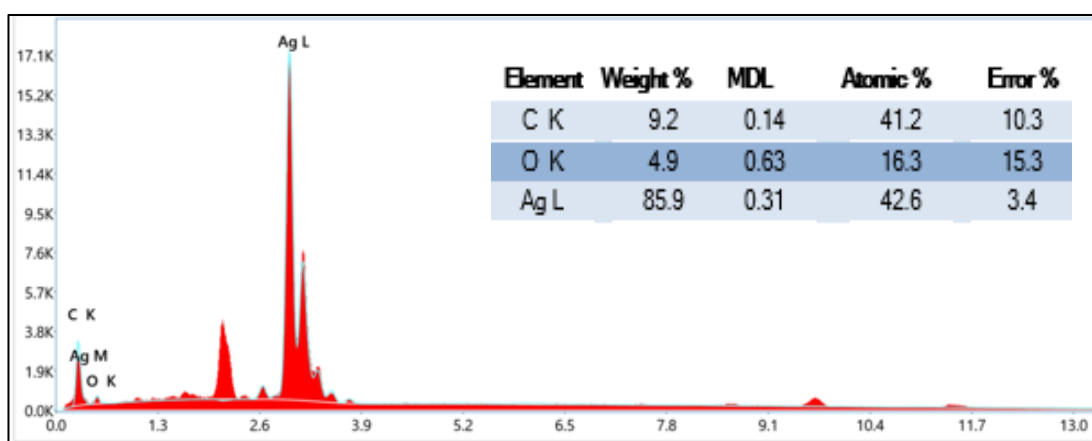


Figure 4. 5. EDS of GO-Ag nanocomposite



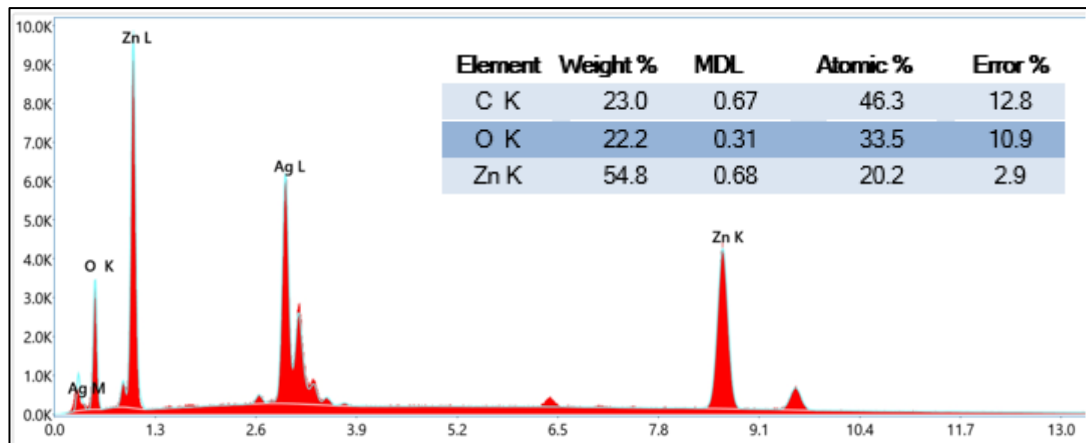


Figure 4. 9. EDS of GO-ZnO nanocomposite

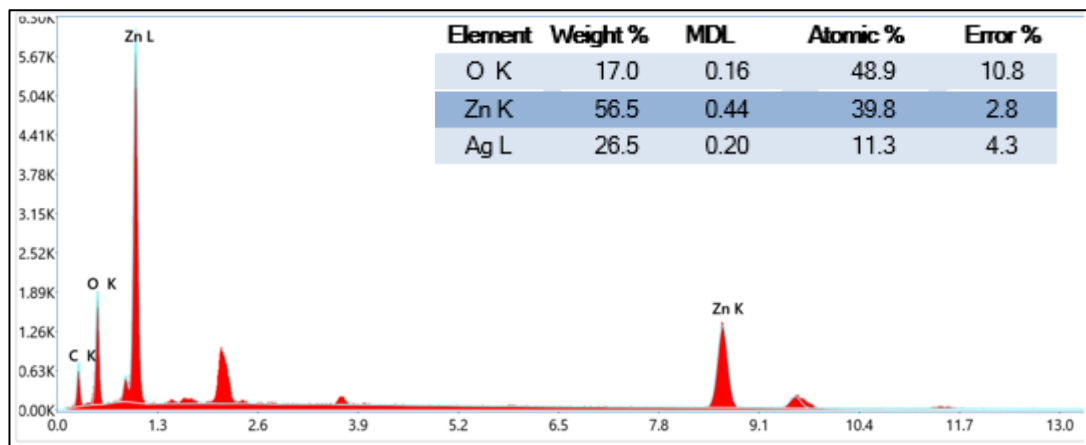


Figure 4. 8. EDS of Ag-ZnO nanocomposite

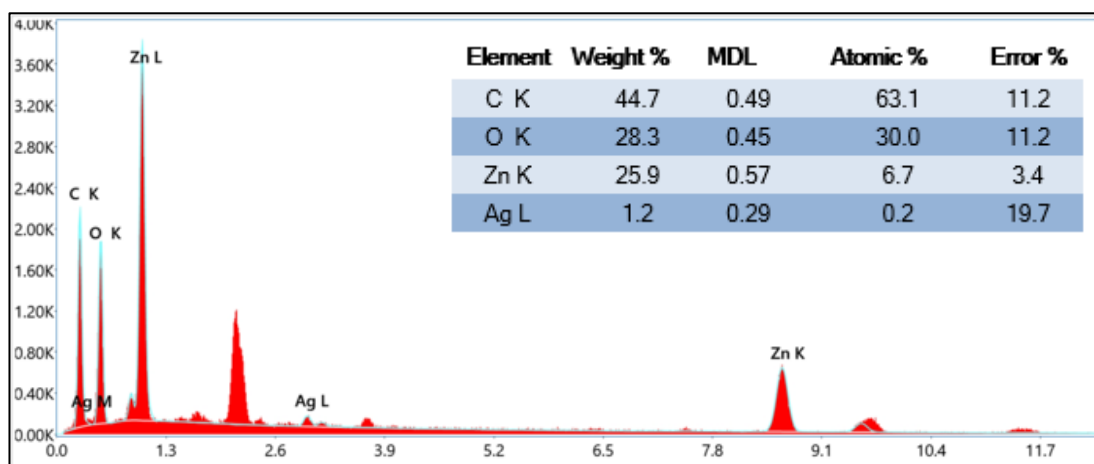


Figure 4. 7. EDS of GO-Ag-ZnO nanocomposite

As we can see in the above EDS analysis done for nanocomposites, All the samples showed the desired peaks necessary for the purity of the synthesized materials. For GO-Ag-ZnO, the peaks associated with Ag, C, O and Zn were observed which confirms that the sample is of high purity.

### **3.4. X-ray diffraction (XRD)**

The XRD patterns for Ag NPs are shown which clearly highlights the anticipated peaks of  $2\theta$  at  $37.6^\circ$ ,  $43.8^\circ$ ,  $63.1^\circ$ ,  $76.9^\circ$ , and  $81.3^\circ$  corresponding to the planes (111), (200), (220), (311), and (222) according to the JCPDs card 04-0783 [82]. The generated ZnO NPs XRD pattern is hexagonal in nature. Peaks that were sharper and more powerful were seen. The diffraction peaks associated with (100), (002), (101), (102), (110), (103), (112), (200), (201) are of  $2\theta$  at  $31.7^\circ$ ,  $34.4^\circ$ ,  $36.2^\circ$ ,  $47.5^\circ$ ,  $56.5^\circ$ ,  $62.8^\circ$ ,  $66.3^\circ$ ,  $67.9^\circ$ ,  $69.0^\circ$ , and  $72.5^\circ$ . (004). JCPDs card 36-1451 was used to confirm the peaks [82]. The XRD pattern observed for GO sheets as synthesized by improved hummer's method. The diffraction peak at  $10.5^\circ$  is of high intensity which confirms the formation of GO having crystal plane of (001). The high purity of ZnO products is demonstrated by the ability of the prepared ZnO NPs diffraction peaks to be precisely matched to the hexagonal phase of ZnO JCPDs card 36-1451. In addition to ZnO diffraction peaks, several peaks at  $38.3^\circ$ ,  $44.2^\circ$ ,  $64.4^\circ$  correlates to the Ag NPs pattern according to the JCPDs card 04-0783, which confirms the formation of Ag-ZnO. [83]. XRD peak of the composite GO-ZnO shows a distinctive peak at  $12.3^\circ$  for graphene oxide, which responds to the crystal plane of the (001) and it also shows the diffraction peaks for ZnO [84]. GO displays a distinct peak at  $11.6^\circ$ , which corresponds to the crystal plane (001). The xrd pattern for GO-Ag, showed that this peak had vanished and that a new, broad peak had appeared at  $20.4^\circ$ , which corresponds to (001), as shown in the Figure. When compared to the published data, the Ag-GO pattern's intense four peaks at  $38.1^\circ$ ,  $44.5^\circ$ ,  $64.6^\circ$ , and  $77.5^\circ$  correlate to the (111), (200), (220), and (311) [85]. The XRD pattern of GO-Ag-ZnO nanocomposite shows the diffraction peaks of ZnO in relation with the standard JCPDs card 36-1451. For Ag the diffractions peaks were at  $37.6^\circ$  and  $43.8^\circ$ , representing the (111) and (200) planes as confirmed by JCPDs card 04-0783. The diffraction peak observed for GO is small, the reason could be the low diffraction intensity or low GO concentration. The XRD pattern confirms the successful synthesis of GO-Ag-ZnO [86].

XRD pattern observed for the deposited thin film samples were not recorded as it would be the same as the powder samples formed. In-situ deposited Ag NPs thin film was subjected to xrd which shows the peak at  $38.1^\circ$ ,  $44.3^\circ$  which corresponds to the planes (111) and (200).

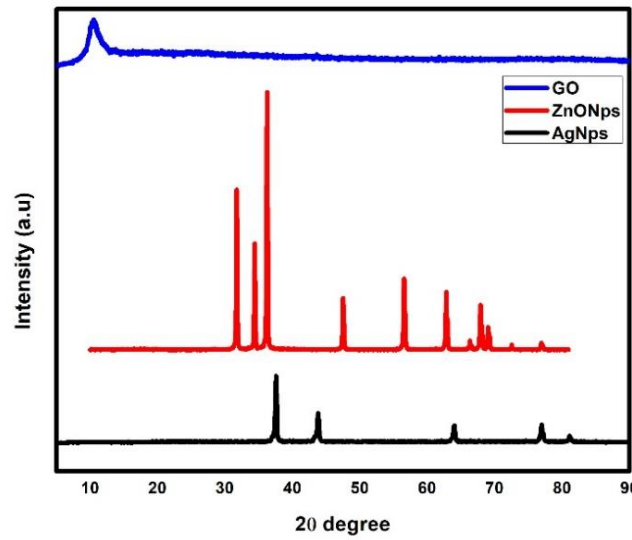


Figure 4. 10. XRD pattern observed for AgNPs, ZnONPs and GO

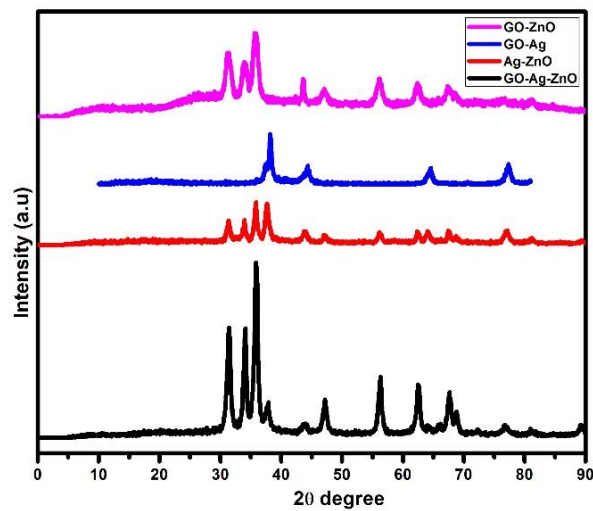


Figure 4. 11. XRD pattern observed for the respective synthesized nanocomposites.

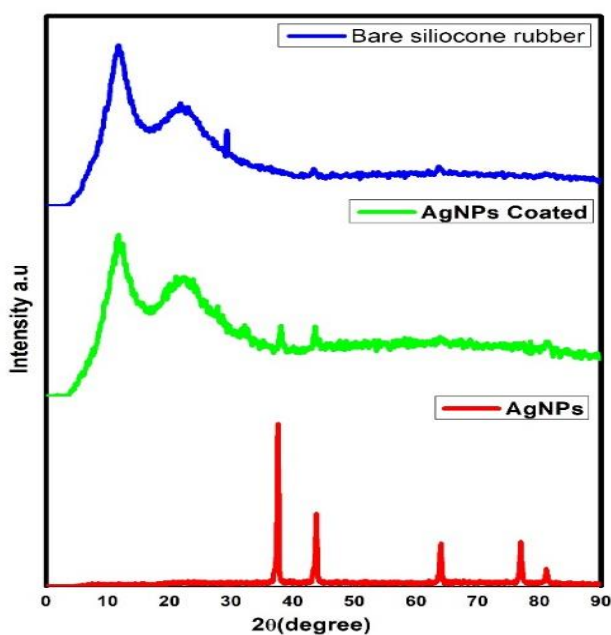


Figure 4. 12. XRD pattern of Bare silicone rubber, In-situ AgNPs coated silicone rubber and AgNPs.

### 3.5. Fourier transform infra-red (FT-IR) spectroscopy.

FTIR **Figure 4.14** shows a broad peak at  $3439\text{cm}^{-1}$  for the synthesized GO-Ag-ZnO, which is the O–H stretching vibrations. Graphene oxide shows a broad band at  $1096\text{cm}^{-1}$ ,  $1634\text{cm}^{-1}$ ,  $1730\text{cm}^{-1}$  which corresponds to the C–O bond [87]. Two identical absorption bands of C=O group were identified here at  $1630\text{cm}^{-1}$  and  $1388\text{cm}^{-1}$ . Around  $589\text{cm}^{-1}$  strong vibrational peaks describe the existence of ZnO NPs. For GO-Ag nanocomposite, the peaks at  $686\text{cm}^{-1}$  may be assigned to Ag NPs which confirms the synthesis of GO-Ag nanocomposite. The FTIR spectrum of synthesized ZnO NPs corresponds to a peak at  $3344\text{cm}^{-1}$  which is due to the presence of oxygen and hydrogen groups. Around  $1020\text{cm}^{-1}$  a large band relates to C–O stretching,  $1567\text{cm}^{-1}$  and  $1419\text{cm}^{-1}$  are the main characteristic bands of ZnO NPs. Peaks assigned at  $643\text{cm}^{-1}$ ,  $578\text{cm}^{-1}$ ,  $429\text{cm}^{-1}$  Zn–O stretching vibrations peaks are assigned at  $643\text{cm}^{-1}$ ,  $578\text{cm}^{-1}$ ,  $429\text{cm}^{-1}$  and  $417\text{cm}^{-1}$ . GO-ZnO nanocomposite FTIR spectra shows the peak at  $1627\text{cm}^{-1}$ ,  $3428\text{cm}^{-1}$  and  $1109\text{cm}^{-1}$  is related to the C=C stretching, O–H stretching and C–OH groups. The peak at  $650\text{cm}^{-1}$  is in relation to the stretching frequency of ZnO, which reveals the presence of ZnO NPs on GO surface **Figure 4.13**. [84] For

the synthesized materials the peaks observed were in relation with the reported literature.

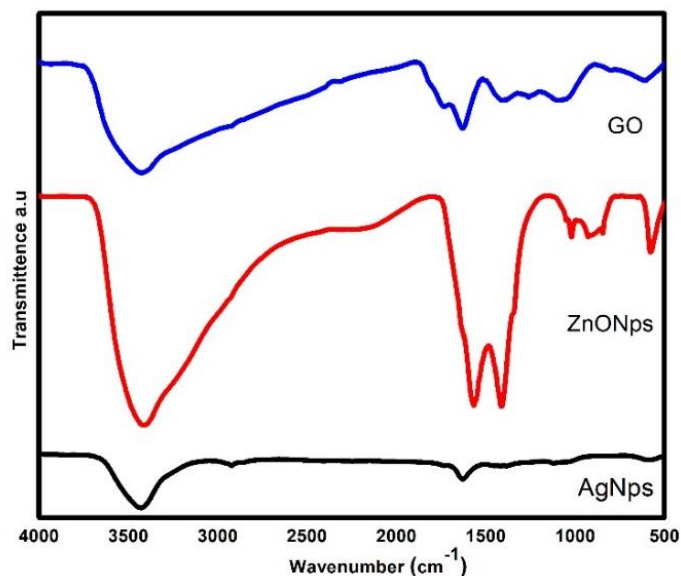


Figure 4. 13. FT-IR spectra of, Ag NPs, ZnO NPs and Graphene oxide GO

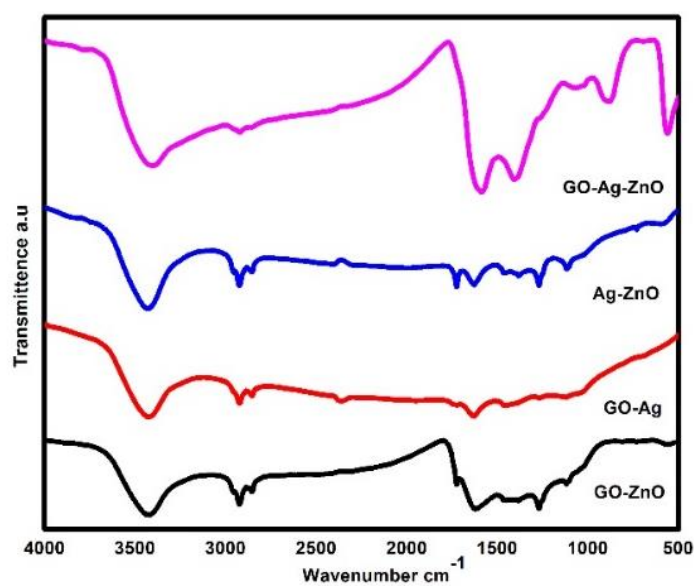


Figure 4. 14. FT-IR spectra of the synthesized nanocomposites.

### 3.6. UV- Vis spectroscopy

All the samples were subjected to UV-vis spectrum in a range of 200nm – 900nm. It was performed to study the structural characterization of AgNPs, ZnONPs, GO, Ag-ZnO, GO-Ag, GO-ZnO and GO-Ag-ZnO nanocomposites. The characteristics like

size and shape depends on the absorbance pattern of the nanomaterials. The solutions of AgNPs, ZnONPs, GO, GO-Ag, GO-ZnO, Ag-ZnO and GO-Ag-ZnO were made using distilled water as a solvent.

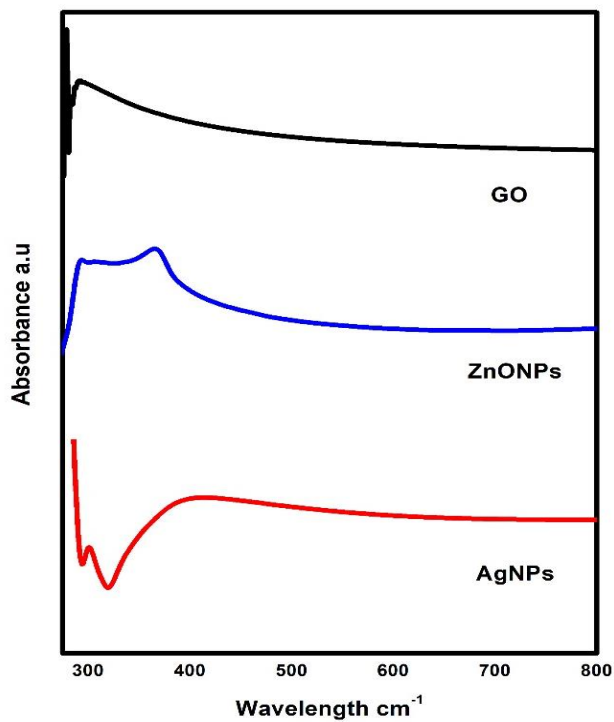


Figure 4. 16. UV-Vis spectrum of AgNPs, ZnONPs and graphene oxide.

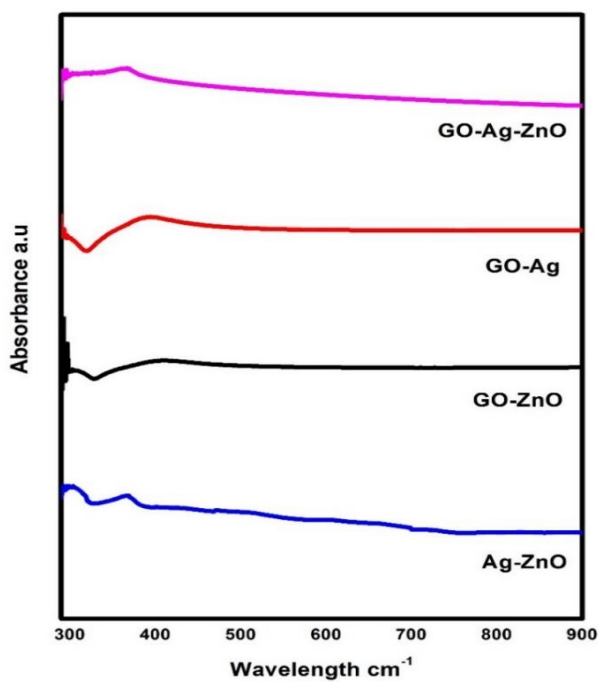


Figure 4. 15. UV-Vis spectrum of the synthesized nanocomposite.

Ag NPs shows absorbance around 400 nm – 420 nm range, ZnO NPs around 390 nm and GO in 290 nm range. GO-ZnO, GO-Ag and Ag-ZnO displayed two characteristics peaks due to the deposition of nanoparticles onto the surface or the formation of nanoparticles. However, GO-Ag-ZnO showed a broad absorption spectrum in the whole region 200nm - 900nm, whereas the strongest absorption peak that was calculated, appeared at the range of less than 400nm.

### 3.7. Contact angle measurement

The surface hydrophilicity and hydrophobicity are measured by contact angle, as it's the measurement between a water droplet and the surface of a polymer/ coated or uncoated. This is performed by using a water drop analyzer, which precisely controls the number of drops to fall onto the surface. Ag NPs coated and GO-Ag-ZnO coated silicone were successfully prepared on plasma treated silicone rubber. For the measurement of the contact angle of a DI water droplet for the uncoated surface, Ag NPs-coated and GO-Ag-ZnO coated surfaces are shown in figure.

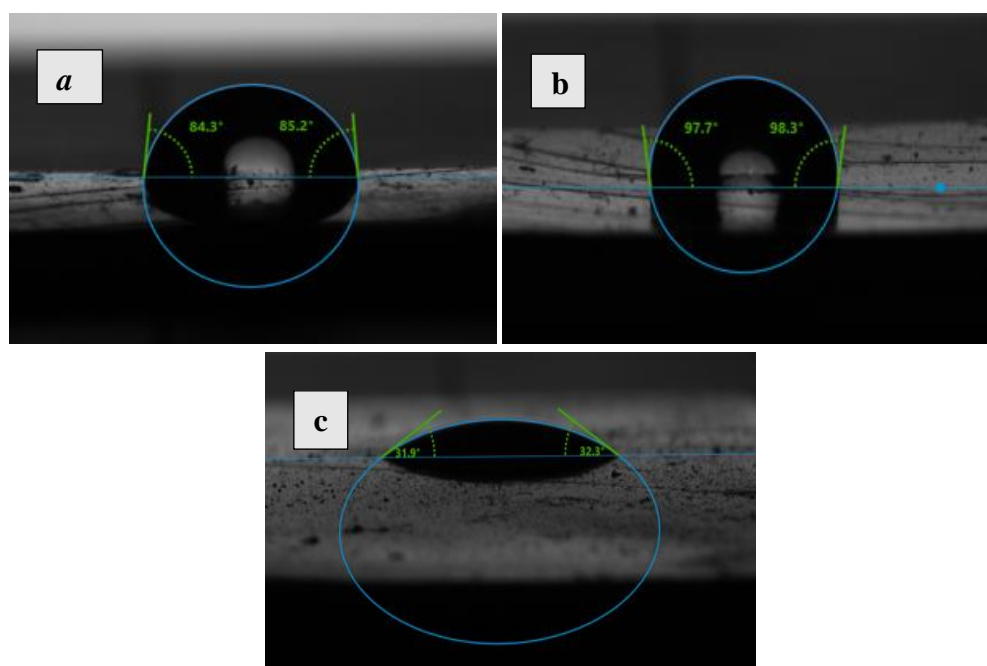


Figure 4. 17. Contact angle measurement of a) bare silicone rubber b) Silver coated silicone rubber c) GO-Ag-ZnO nanocomposite coated silicone rubber

The water contact angle of bare silicone rubber was hydrophobic in nature and the Ag NPs-coated ( $\sim 91.7^\circ$ ) shows  $WCA > 90$ , which indicates the hydrophobic characteristics of the material. Whereas the WCA of GO-Ag-ZnO nanocomposite ( $\sim 31.9^\circ$ ) is  $< 90$  which indicates the hydrophilicity of our material. In general, a hydrophilic coating is often applied to urinary catheters to improve their lubricity and reduce friction during insertion and removal. Surfaces having a contact angle of  $54 - 130^\circ$  due to the increase of hydrophobic interactions between the bacterial membrane and the solid surface, the bacterial adherence was also increased [88]. The surfaces having normal range of wettability are more able to bind the bacterial cells [89].

### **3.8. Antibacterial activity of synthesized materials**

The intention of our study was to find out the antibacterial activity of the synthesized Ag NPs, ZnO NPs, GO, Ag-ZnO, GO-ZnO, GO-Ag, GO-Ag-ZnO nanocomposites. The Kirby-Bauer method was used to evaluate the antibacterial assay of the synthesized materials against human pathogenic. To study the antibacterial activity, two bacterial strains were chosen including *Escherichia coli* (*E. coli*) and *Staphylococcus aureus* (*S. aureus*). The zone of inhibition (ZOI) against these bacterial strains were achieved in the following order  $GO > ZnO > Ag > \text{sample 3} > \text{sample 2} > \text{sample 1} > GO-Ag-ZnO$ . The zone of inhibition produced by Ag, ZnO, GO, sample 2, sample 3, sample 1 and GO-Ag-ZnO showed in the following range, 7-9mm, 6.5-8mm, 7-8mm, 6-9mm, 6.5-8mm, 8-11mm and 8-14mm.

#### **3.8.1. Agar dilution method**

The Agar-well diffusion method with Luria Bertani (LB) growth media was used for the assessment of the antibacterial activity of the synthesized materials. The pH of the LB broth was adjusted to 7–7.5 before it was autoclaved.

Serial dilutions of the prepared AgNPs, ZnONPs, GO, sample 1, sample 2, sample 3, GO-Ag-ZnO nanocomposites with concentration 2mg, 1mg and 0.5mg, was dispersed separately in 1ml of DI water. After that, sterile petri plates were filled with the agar and let to set. Bacterial strains were freshly cultured, around 50  $\mu\text{l}$  of bacteria were dropped onto the agar plates. Then the drop of bacterial culture was spread on the plates using a sterilized cotton swab. The disk diffusion method was used for testing the bactericidal presence in the disks impregnated with the samples of different



concentrations. Each well's bacterial ZOI was measured separately, and the diameter of each zone was noted in millimeters (mm). The zone of inhibition results for each sample is given below in the table.

*Table 4. 1 ZOI values of Ag, ZnO, GO, sample 1, sample 2, sample 3 and GO-Ag-ZnO nanocomposite against G+ and G- bacterial strains.*

S.NO	Materials	Zone of inhibition (in mm)		
		(mg/ml)	Staphylococcus aureus	Escherichia coli
1	Ag NPs	2mg	9mm	9mm
		1mg	8mm	7mm
		0.5	7.5 mm	6.5mm
2	ZnONPs	2mg	8mm	8mm
		1mg	7mm	8mm
		0.5mg	6.5mm	7mm
3	GO	2mg	8mm	8mm
		1mg	6.5mm	8mm
		0.5mg	6.5mm	6.5mm

Table 4. 2 ZOI values of Ag, ZnO, GO, sample 1, sample 2, sample 3 and GO-Ag-ZnO nanocomposite against G+ and G- bacterial strains.

S.NO	Materials	(mg/l)	Zone of inhibition (in mm)	
			Staphylococcus aureus	Escherichia coli
4	Ag-ZnO	2mg	11mm	9mm
		1mg	10mm	9mm
		0.5mg	8mm	8mm
5	GO-Ag	2mg	7mm	9mm
		1mg	7mm	9mm
		0.5mg	6.5mm	7mm
6	GO-ZnO	2mg	8mm	8mm
		1mg	7mm	8mm
		0.5mg	7mm	7mm
7	GO-Ag-ZnO	2mg	14mm	11mm
		1mg	12mm	10mm
		0.5mg	8mm	8mm

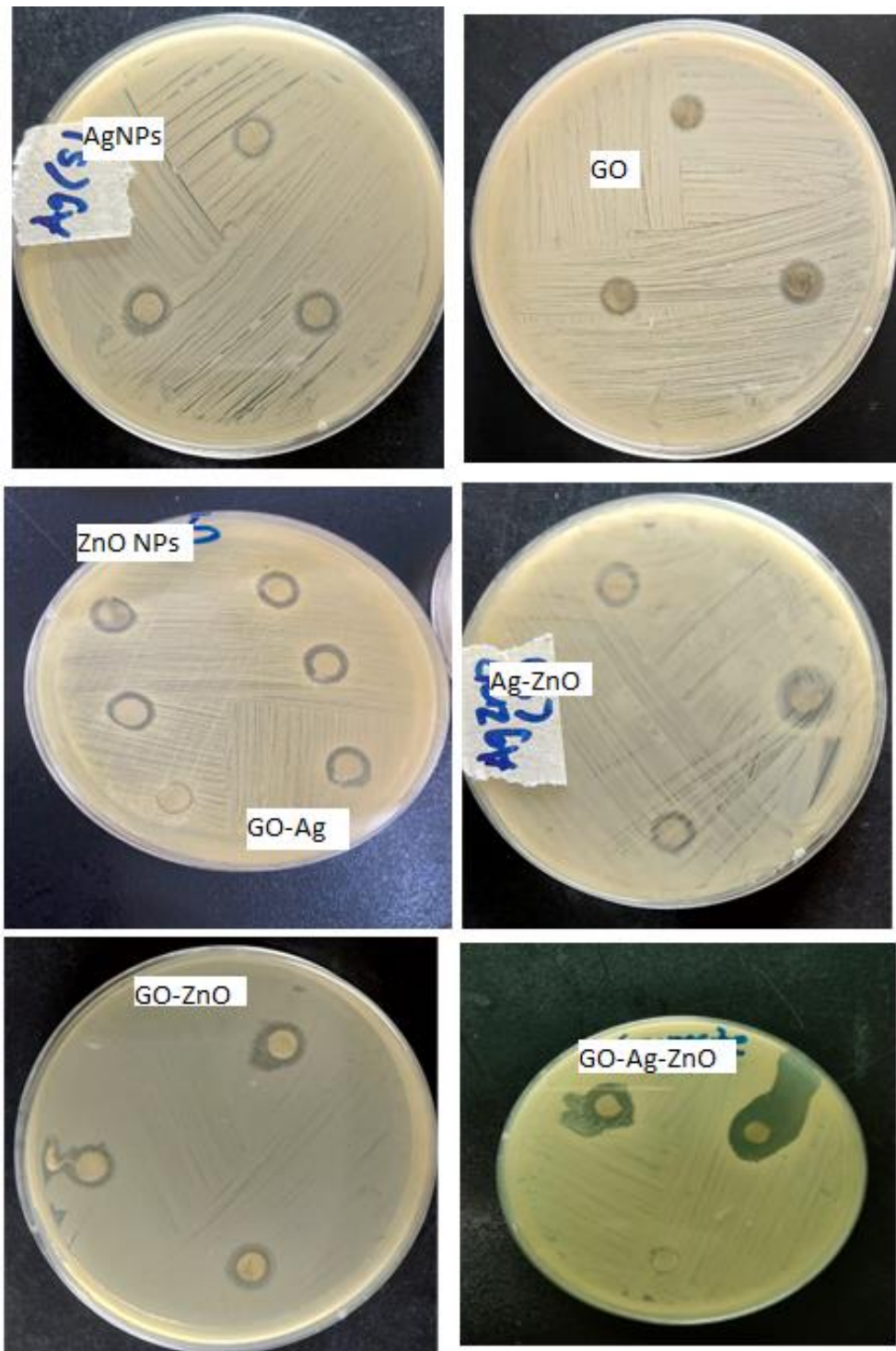


Figure 4. 18. Zone of inhibition values of Ag, ZnO, GO, sample 1, sample 2, sample 3 and GO-Ag-ZnO nanocomposite against *S. aureus*.

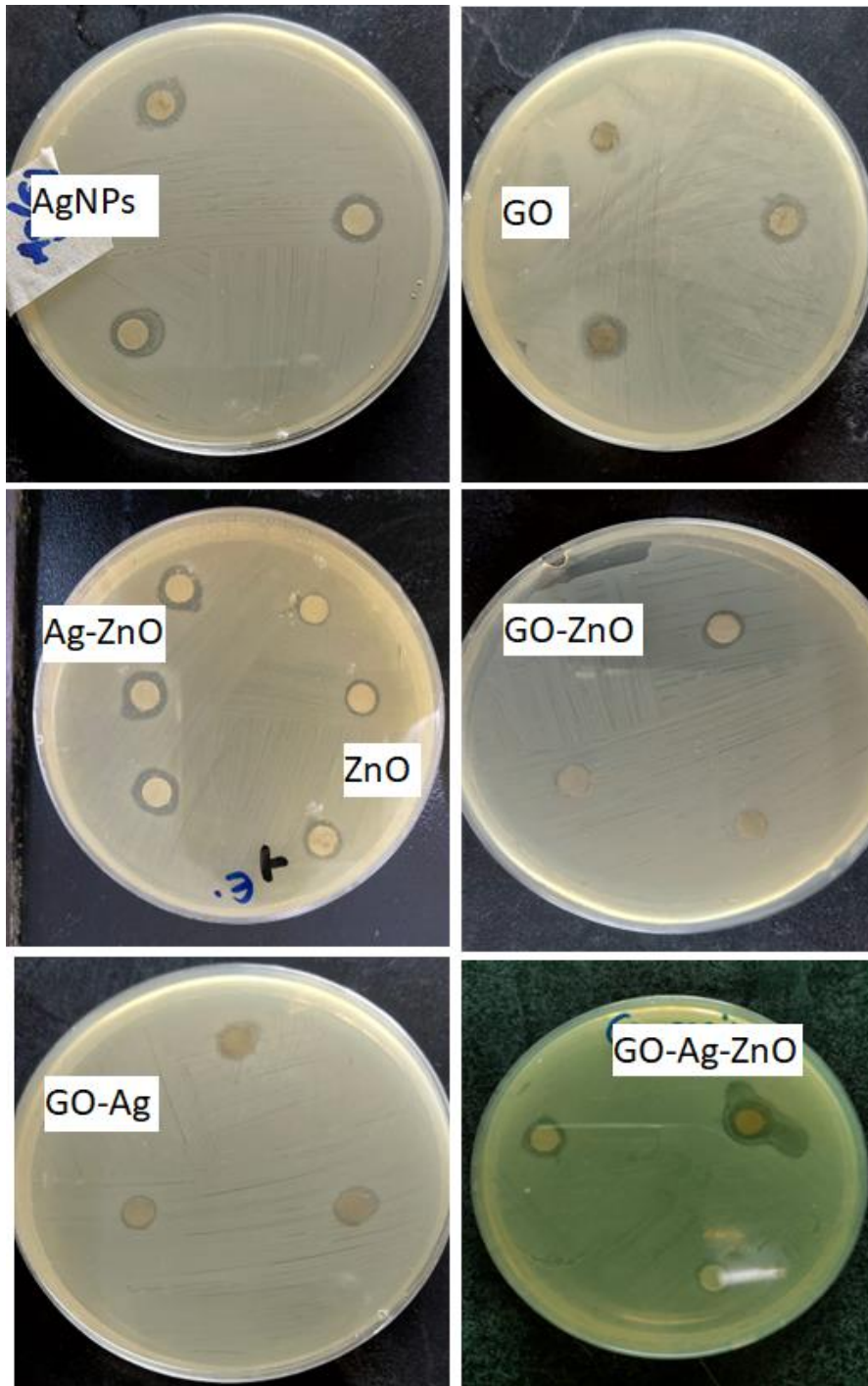


Figure 4. 19. ZOI values of Ag, ZnO, GO, sample 1, sample 2, sample 3 and GO-Ag-ZnO nanocomposite against *E. coli*

### **3.8.2. Minimum inhibitory concentration MIC determination**

An antibacterial agent that stops or inhibits the growth of a microorganism at a very low concentration is known as minimum inhibitory concentration MIC. The Ag NPs and GO-Ag-ZnO nanocomposite antibacterial effectiveness was investigated using the common broth dilution method (CLSI M07-A8). In a liquid growth medium various concentrations of bacteria are introduced, and the results are frequently recorded. After incubation for a defined amount of time (16–24 hours), growth is evaluated, and the MIC value is read.

Adjusted bacterial concentrations and successive two-fold dilutions of the sample Ag NPs and GO-Ag-ZnO nanocomposite ranging from 0.5 mg/mL - 0.156 mg/mL were used to determine the MIC. These dilutions along with the controlled sample containing inoculated broth was incubated for 1 day (24hrs) at 37°C. The MIC endpoint is the concentration of nanocomposites at which there is no visible growth in the tubes. The visual turbidity of the tubes were measured before and after confirm the MIC value, the visual turbidity of the tubes was measured both before and after incubation.

### **3.8.3. Minimum bactericidal concentration MBC determination**

After the determination of MIC for GO-Ag-ZnO nanocomposite and Ag NPs, MBC was calculated. Aliquots of 50µl from every tube that had no discernible bacterial growth was placed on the plates with the poured agar solution and incubated at 37 °C for 1 day. MBC endpoint occurs when the least amount of the antibacterial agent eliminates 99.9% of the bacterial population. This was accomplished by checking agar plates that had been pre- and post-incubated to see if any bacteria were present.

**Minimum inhibitory concentration MIC and Minimum bactericidal concentration MBC values against E. coli:**

*Table 4. 3. Ag NPs and GO-Ag-ZnO nanocomposite MIC and MBC values*

No	Sample name	MIC value	MBC value	Standard reported value
1	AgNPs	0.25mg/ml	1 mg/ml	MIC 2.5mg/ml [90]
7	GO-Ag-ZnO	0.125mg/ml	0.25mg/ml	MBC 5mg/ml, 0.02mg/ml [91, 92]

**Minimum inhibitory concentration MIC and Minimum bactericidal concentration MBC values against E. coli:**

*Table 4. 4. Ag NPs and GO-Ag-ZnO nanocomposite MIC and MBC values*

No	Sample name	MIC value	MBC value	Standard reported values
1	AgNPS	0.5mg/ml	1.5mg/ml	MIC 3.1mg/ml [90]
7	GO-Ag-ZnO	0.125mg/ml	0.25mg/ml	MBC 0.625mg/ml[93]

## Conclusion

Herein, GO-Ag-ZnO based nanocomposite was prepared as an antibacterial agent to enhance the antibacterial activity of the polymeric hospitalities and its characterization has been completed. The characterization techniques revealed a good interaction and compatibility between GO, Ag NPs and ZnO NPs. The properties of the synthesized antibacterial agent were carefully assessed and compared with that of the individual components as well. The silicone substrate was coated with GO-Ag-ZnO through a simple spin coating technique with the help of PVA as a binder. The results showed that the synthesized GO-Ag-ZnO has a significant antibacterial activity against gram +ve and gram -ve bacteria and that this could be a promising candidate for the development of long lasting, high efficiency antibacterial coatings for urinary catheters. The study also confirmed that the hydrophilic nature of our material is in accordance with the literature reported.

Further exploration can lead to better and improved results by the optimization and study of the composite coating factors, release of ions and cell cytotoxicity can be explored for its practical use.

## References

- [1] S. Saint, J. Wiese, J. K. Amory, M. L. Bernstein, U. D. Patel, J. K. Zemencuk, *et al.*, "Are physicians aware of which of their patients have indwelling urinary catheters?," *The American journal of medicine*, vol. 109, pp. 476-480,(2000).
- [2] J. W. Weinstein, D. Mazon, E. Pantelick, P. Reagan-Cirincione, L. M. Dembry, and W. J. Hierholzer, "A decade of prevalence surveys in a tertiary-care center: trends in nosocomial infection rates, device utilization, and patient acuity," *Infection Control & Hospital Epidemiology*, vol. 20, pp. 543-548, (1999).
- [3] M. T. Greene, M. G. Fakhri, K. E. Fowler, J. Meddings, D. Ratz, N. Safdar, *et al.*, "Regional variation in urinary catheter use and catheter-associated urinary tract infection: results from a national collaborative," *Infection Control & Hospital Epidemiology*, vol. 35, pp. S99-S106, (2014).
- [4] C. V. Gould, C. A. Umscheid, R. K. Agarwal, G. Kuntz, D. A. Pegues, and H. I. C. P. A. Committee, "Guideline for prevention of catheter-associated urinary tract infections 2009," *Infection Control & Hospital Epidemiology*, vol. 31, pp. 319-326, (2010).
- [5] R. L. Munasinghe, H. Yazdani, M. Siddique, and W. Hafeez, "Appropriateness of use of indwelling urinary catheters in patients admitted to the medical service," *Infection Control & Hospital Epidemiology*, vol. 22, pp. 647-649, (2001).
- [6] K. Schumm and T. B. Lam, "Types of urethral catheters for management of short-term voiding problems in hospitalised adults," *Cochrane Database of Systematic Reviews*, (2008).
- [7] E. Lo, L. E. Nicolle, S. E. Coffin, C. Gould, L. L. Maragakis, J. Meddings, *et al.*, "Strategies to prevent catheter-associated urinary tract infections in acute care hospitals: 2014 update," *Infection Control & Hospital Epidemiology*, vol. 35, pp. 464-479, (2014).
- [8] S. Saint and C. E. Chenoweth, "Biofilms and catheter-associated urinary tract infections," *Infectious Disease Clinics*, vol. 17, pp. 411-432, (2003).
- [9] D. J. Durant, "Nurse-driven protocols and the prevention of catheter-associated urinary tract infections: a systematic review," *American journal of infection control*, vol. 45, pp. 1331-1341, (2017).
- [10] T. B. Lam, M. I. Omar, E. Fisher, K. Gillies, and S. MacLennan, "Types of indwelling urethral catheters for short-term catheterisation in hospitalised adults," *Cochrane Database of Systematic Reviews*, (2014).



- [11] M. Ruutu, O. Alfthan, M. Talja, and L. Andersson, "Cytotoxicity of latex urinary catheters," *British journal of urology*, vol. 57, pp. 82-87, (1985).
- [12] J. Stensballe, D. Looms, P. Nielsen, and M. Tvede, "Hydrophilic-coated catheters for intermittent catheterisation reduce urethral micro trauma: a prospective, randomised, participant-blinded, crossover study of three different types of catheters," *European Urology*, vol. 48, pp. 978-983, (2005).
- [13] I. Francolini, C. Vuotto, A. Piozzi, and G. Donelli, "Antifouling and antimicrobial biomaterials: an overview," *Apmis*, vol. 125, pp. 392-417, (2017).
- [14] Z. Zhu, Z. Wang, S. Li, and X. Yuan, "Antimicrobial strategies for urinary catheters," *Journal of Biomedical Materials Research Part A*, vol. 107, pp. 445-467, (2019).
- [15] J. P. Jinhuan Jiang, 1 and Jiye Caicorresponding author 1, 2, "The Advancing of Zinc Oxide Nanoparticles for Biomedical Applications," *Bioinorganic chemistry and application*, (2018).
- [16] T. Theivasanthi and M. Alagar, "Electrolytic synthesis and characterizations of silver nanopowder," *arXiv preprint arXiv:1111.0260*, (2011).
- [17] A. B. Lansdown, "A pharmacological and toxicological profile of silver as an antimicrobial agent in medical devices," *Advances in pharmacological sciences*, vol. (2010), 2010.
- [18] C. F. Jones and D. W. Grainger, "In vitro assessments of nanomaterial toxicity," *Advanced drug delivery reviews*, vol. 61, pp. 438-456, (2009).
- [19] S. Prabhu and E. K. Poullose, "Silver nanoparticles: mechanism of antimicrobial action, synthesis, medical applications, and toxicity effects," *International nano letters*, vol. 2, pp. 1-10, (2012).
- [20] K. Chaloupka, Y. Malam, and A. M. Seifalian, "Nanosilver as a new generation of nanoparticle in biomedical applications," *Trends in biotechnology*, vol. 28, pp. 580-588, (2010).
- [21] P. Asharani, M. P. Hande, and S. Valiyaveetil, "Anti-proliferative activity of silver nanoparticles," *BMC cell biology*, vol. 10, pp. 1-14, (2009).
- [22] O. Choi, K. K. Deng, N.-J. Kim, L. Ross Jr, R. Y. Surampalli, and Z. Hu, "The inhibitory effects of silver nanoparticles, silver ions, and silver chloride colloids on microbial growth," *Water research*, vol. 42, pp. 3066-3074, (2008).
- [23] J. R. Morones, J. L. Elechiguerra, A. Camacho, K. Holt, J. B. Kouri, J. T. Ramírez, *et al.*, "The bactericidal effect of silver nanoparticles," *Nanotechnology*, vol. 16, p. 2346, (2005).
- [24] J. S. Kim, E. Kuk, K. N. Yu, J.-H. Kim, S. J. Park, H. J. Lee, *et al.*, "Antimicrobial effects of silver nanoparticles," *Nanomedicine: Nanotechnology, biology and medicine*, vol. 3, pp. 95-101, (2007).

- [25] X. H. Vu, T. T. T. Duong, T. T. H. Pham, D. K. Trinh, X. H. Nguyen, and V.-S. Dang, "Synthesis and study of silver nanoparticles for antibacterial activity against *Escherichia coli* and *Staphylococcus aureus*," *Advances in Natural Sciences: Nanoscience and Nanotechnology*, vol. 9, p. 025019, (2018).
- [26] J. Li, K. Rong, H. Zhao, F. Li, Z. Lu, and R. Chen, "Highly selective antibacterial activities of silver nanoparticles against *Bacillus subtilis*," *Journal of Nanoscience and Nanotechnology*, vol. 13, pp. 6806-6813, (2013).
- [27] H. Xu, F. Qu, H. Xu, W. Lai, Y. Andrew Wang, Z. P. Aguilar, *et al.*, "Role of reactive oxygen species in the antibacterial mechanism of silver nanoparticles on *Escherichia coli* O157: H7," *Biometals*, vol. 25, pp. 45-53, (2012).
- [28] R. Zia, M. Riaz, N. Farooq, A. Qamar, and S. Anjum, "Antibacterial activity of Ag and Cu nanoparticles synthesized by chemical reduction method: a comparative analysis," *Materials Research Express*, vol. 5, p. 075012, (2018).
- [29] E. Z. Gomaa, "Silver nanoparticles as an antimicrobial agent: A case study on *Staphylococcus aureus* and *Escherichia coli* as models for Gram-positive and Gram-negative bacteria," *The Journal of general and applied microbiology*, vol. 63, pp. 36-43, (2017).
- [30] Y. Xie, Y. He, P. L. Irwin, T. Jin, and X. Shi, "Antibacterial activity and mechanism of action of zinc oxide nanoparticles against *Campylobacter jejuni*," *Applied and environmental microbiology*, vol. 77, pp. 2325-2331, (2011).
- [31] R. Brayner, R. Ferrari-Iliou, N. Brivois, S. Djediat, M. F. Benedetti, and F. Fiévet, "Toxicological impact studies based on *Escherichia coli* bacteria in ultrafine ZnO nanoparticles colloidal medium," *Nano letters*, vol. 6, pp. 866-870, (2006).
- [32] M. Li, L. Zhu, and D. Lin, "Toxicity of ZnO nanoparticles to *Escherichia coli*: mechanism and the influence of medium components," *Environmental science & technology*, vol. 45, pp. 1977-1983, (2011).
- [33] A. Lipovsky, Y. Nitzan, A. Gedanken, and R. Lubart, "Antifungal activity of ZnO nanoparticles—the role of ROS mediated cell injury," *Nanotechnology*, vol. 22, p. 105101, (2011).
- [34] J. Sawai, S. Shoji, H. Igarashi, A. Hashimoto, T. Kokugan, M. Shimizu, *et al.*, "Hydrogen peroxide as an antibacterial factor in zinc oxide powder slurry," *Journal of fermentation and bioengineering*, vol. 86, pp. 521-522, (1998).
- [35] K. Kasemets, A. Ivask, H.-C. Dubourguier, and A. Kahru, "Toxicity of nanoparticles of ZnO, CuO and TiO<sub>2</sub> to yeast *Saccharomyces cerevisiae*," *Toxicology in vitro*, vol. 23, pp. 1116-1122, (2009).
- [36] J. Pasquet, Y. Chevalier, E. Couval, D. Bouvier, and M.-A. Bolzinger, "Zinc oxide as a new antimicrobial preservative of topical products: Interactions with common

- formulation ingredients," *International journal of pharmaceutics*, vol. 479, pp. 88-95, (2015).
- [37] L. Zhang, Y. Ding, M. Povey, and D. York, "ZnO nanofluids—A potential antibacterial agent," *Progress in Natural Science*, vol. 18, pp. 939-944, (2008).
- [38] J. L. Venkataraju, R. Sharath, M. Chandraprabha, E. Neelufar, A. Hazra, and M. Patra, "Synthesis, characterization and evaluation of antimicrobial activity of zinc oxide nanoparticles," *Journal of Biochemical Technology*, vol. 3, pp. 151-154, (2014).
- [39] D. Manyasree, P. Kiranmayi, and R. K. Venkata, "Characterization and antibacterial activity of ZnO nanoparticles synthesized by co-precipitation method," *Int J App Pharm*, vol. 10, pp. 224-228, (2018).
- [40] M. Alekish, Z. B. Ismail, B. Albiss, and S. Nawasrah, "In vitro antibacterial effects of zinc oxide nanoparticles on multiple drug-resistant strains of *Staphylococcus aureus* and *Escherichia coli*: An alternative approach for antibacterial therapy of mastitis in sheep," *Veterinary world*, vol. 11, p. 1428, (2018).
- [41] A. H. Ali, "Experimental investigations on effects of ZnO NPS and annona muricata extract for in vitro and in vivo antibacterial activity," *Materials Today: Proceedings*, vol. 57, pp. 527-530, (2022).
- [42] K. S. Novoselov, A. K. Geim, S. V. Morozov, D.-e. Jiang, Y. Zhang, S. V. Dubonos, *et al.*, "Electric field effect in atomically thin carbon films," *science*, vol. 306, pp. 666-669, (2004).
- [43] H. Y. Mao, S. Laurent, W. Chen, O. Akhavan, M. Imani, A. A. Ashkarran, *et al.*, "Graphene: promises, facts, opportunities, and challenges in nanomedicine," *Chemical reviews*, vol. 113, pp. 3407-3424, (2013).
- [44] X.-Q. Wei, L.-Y. Hao, X.-R. Shao, Q. Zhang, X.-Q. Jia, Z.-R. Zhang, *et al.*, "Insight into the interaction of graphene oxide with serum proteins and the impact of the degree of reduction and concentration," *ACS applied materials & interfaces*, vol. 7, pp. 13367-13374, (2015).
- [45] J. Liu, J. Dong, T. Zhang, and Q. Peng, "Graphene-based nanomaterials and their potentials in advanced drug delivery and cancer therapy," *Journal of Controlled Release*, vol. 286, pp. 64-73, (2018).
- [46] J. Kim, K. S. Choi, Y. Kim, K. T. Lim, H. Seonwoo, Y. Park, *et al.*, "Bioactive effects of graphene oxide cell culture substratum on structure and function of human adipose-derived stem cells," *Journal of Biomedical Materials Research Part A: An Official Journal of The Society for Biomaterials, The Japanese Society for Biomaterials, and The Australian Society for Biomaterials and the Korean Society for Biomaterials*, vol. 101, pp. 3520-3530, (2013).

- [47] K. Yang, S. Zhang, G. Zhang, X. Sun, S.-T. Lee, and Z. Liu, "Graphene in mice: ultrahigh in vivo tumor uptake and efficient photothermal therapy," *Nano letters*, vol. 10, pp. 3318-3323, (2010).
- [48] J. He, X. Zhu, Z. Qi, C. Wang, X. Mao, C. Zhu, *et al.*, "Killing dental pathogens using antibacterial graphene oxide," *ACS applied materials & interfaces*, vol. 7, pp. 5605-5611, (2015).
- [49] K. E. Jones, N. G. Patel, M. A. Levy, A. Storeygard, D. Balk, J. L. Gittleman, *et al.*, "Global trends in emerging infectious diseases," *Nature*, vol. 451, pp. 990-993, 2008.
- [50] O. Akhavan and E. Ghaderi, "Toxicity of graphene and graphene oxide nanowalls against bacteria," *ACS nano*, vol. 4, pp. 5731-5736, (2010).
- [51] S. Liu, T. H. Zeng, M. Hofmann, E. Burcombe, J. Wei, R. Jiang, *et al.*, "Antibacterial activity of graphite, graphite oxide, graphene oxide, and reduced graphene oxide: membrane and oxidative stress," *ACS nano*, vol. 5, pp. 6971-6980, (2011).
- [52] M. Dallavalle, M. Calvaresi, A. Bottoni, M. Melle-Franco, and F. Zerbetto, "Graphene can wreak havoc with cell membranes," *ACS applied materials & interfaces*, vol. 7, pp. 4406-4414, (2015).
- [53] D. R. Dreyer, S. Park, C. W. Bielawski, and R. S. Ruoff, "The chemistry of graphene oxide," *Chemical society reviews*, vol. 39, pp. 228-240, (2010).
- [54] O. N. Ruiz, K. S. Fernando, B. Wang, N. A. Brown, P. G. Luo, N. D. McNamara, *et al.*, "Graphene oxide: a nonspecific enhancer of cellular growth," *ACS nano*, vol. 5, pp. 8100-8107, (2011).
- [55] C. K. Chua, Z. Sofer, and M. Pumera, "Graphite oxides: effects of permanganate and chlorate oxidants on the oxygen composition," *Chemistry—A European Journal*, vol. 18, pp. 13453-13459, (2012).
- [56] W. Hu, C. Peng, W. Luo, M. Lv, X. Li, D. Li, *et al.*, "Graphene-based antibacterial paper," *ACS nano*, vol. 4, pp. 4317-4323, (2010).
- [57] V. T. Pham, V. K. Truong, M. D. Quinn, S. M. Notley, Y. Guo, V. A. Baulin, *et al.*, "Graphene induces formation of pores that kill spherical and rod-shaped bacteria," *ACS nano*, vol. 9, pp. 8458-8467, (2015).
- [58] T. A. Tabish, S. Zhang, and P. G. Winyard, "Developing the next generation of graphene-based platforms for cancer therapeutics: The potential role of reactive oxygen species," *Redox biology*, vol. 15, pp. 34-40, (2018).
- [59] S. Liu, M. Hu, T. H. Zeng, R. Wu, R. Jiang, J. Wei, *et al.*, "Lateral dimension-dependent antibacterial activity of graphene oxide sheets," *Langmuir*, vol. 28, pp. 12364-12372, (2012).
- [60] R. R. Ghanim, M. Mohammad, and A. M. A. Hussien, "Antibacterial Activity and Morphological Characterization of Synthesis Graphene Oxide Nanosheets by

- Simplified Hummer's Method," *Biosciences Biotechnology Research Asia*, vol. 15, p. 627, (2018).
- [61] Q. Bao, D. Zhang, and P. Qi, "Synthesis and characterization of silver nanoparticle and graphene oxide nanosheet composites as a bactericidal agent for water disinfection," *Journal of colloid and interface science*, vol. 360, pp. 463-470, (2011).
- [62] Y. Liu, J. Wen, Y. Gao, T. Li, H. Wang, H. Yan, *et al.*, "Antibacterial graphene oxide coatings on polymer substrate," *Applied Surface Science*, vol. 436, pp. 624-630, (2018).
- [63] K. He, Z. Zeng, A. Chen, G. Zeng, R. Xiao, P. Xu, *et al.*, "Advancement of Ag-graphene based nanocomposites: an overview of synthesis and its applications," *Small*, vol. 14, p. 1800871, (2018).
- [64] W. K. Jung, H. C. Koo, K. W. Kim, S. Shin, S. H. Kim, and Y. H. Park, "Antibacterial activity and mechanism of action of the silver ion in Staphylococcus aureus and Escherichia coli," *Applied and environmental microbiology*, vol. 74, pp. 2171-2178, (2008).
- [65] S. Barua, S. Thakur, L. Aidew, A. K. Buragohain, P. Chattopadhyay, and N. Karak, "One step preparation of a biocompatible, antimicrobial reduced graphene oxide-silver nanohybrid as a topical antimicrobial agent," *RSC Advances*, vol. 4, pp. 9777-9783, (2014).
- [66] A. C. M. de Moraes, B. A. Lima, A. F. de Faria, M. Brocchi, and O. L. Alves, "Graphene oxide-silver nanocomposite as a promising biocidal agent against methicillin-resistant Staphylococcus aureus," *International journal of nanomedicine*, vol. 10, p. 6847, (2015).
- [67] Z. Zhu, M. Su, L. Ma, L. Ma, D. Liu, and Z. Wang, "Preparation of graphene oxide-silver nanoparticle nanohybrids with highly antibacterial capability," *Talanta*, vol. 117, pp. 449-455, (2013).
- [68] S. Archana, K. Y. Kumar, B. Jayanna, S. Olivera, A. Anand, M. Prashanth, *et al.*, "Versatile graphene oxide decorated by star shaped zinc oxide nanocomposites with superior adsorption capacity and antimicrobial activity," *Journal of Science: Advanced Materials and Devices*, vol. 3, pp. 167-174, (2018).
- [69] Y.-W. Wang, A. Cao, Y. Jiang, X. Zhang, J.-H. Liu, Y. Liu, *et al.*, "Superior antibacterial activity of zinc oxide/graphene oxide composites originating from high zinc concentration localized around bacteria," *ACS applied materials & interfaces*, vol. 6, pp. 2791-2798, (2014).
- [70] A. K. Barui, R. Kotcherlakota, and C. R. Patra, "Biomedical applications of zinc oxide nanoparticles," in *Inorganic frameworks as smart nanomedicines*, ed: Elsevier, (2018), pp. 239-278.

- [71] J. Tang, Q. Chen, L. Xu, S. Zhang, L. Feng, L. Cheng, *et al.*, "Graphene oxide–silver nanocomposite as a highly effective antibacterial agent with species-specific mechanisms," *ACS applied materials & interfaces*, vol. 5, pp. 3867-3874, (2013).
- [72] W. Shao, X. Liu, H. Min, G. Dong, Q. Feng, and S. Zuo, "Preparation, characterization, and antibacterial activity of silver nanoparticle-decorated graphene oxide nanocomposite," *ACS applied materials & interfaces*, vol. 7, pp. 6966-6973, (2015).
- [73] D. Prema, J. Prakash, S. Vignesh, P. Veluchamy, C. Ramachandran, D. B. Samal, *et al.*, "Mechanism of inhibition of graphene oxide/zinc oxide nanocomposite against wound infection causing pathogens," *Applied Nanoscience*, vol. 10, pp. 827-849, (2020).
- [74] S. Wang, J. Wu, H. Yang, X. Liu, Q. Huang, and Z. Lu, "Antibacterial activity and mechanism of Ag/ZnO nanocomposite against anaerobic oral pathogen *Streptococcus mutans*," *Journal of Materials Science: Materials in Medicine*, vol. 28, pp. 1-8, (2017).
- [75] N. Agasti and N. Kaushik, "One pot synthesis of crystalline silver nanoparticles," *American Journal of Nanomaterials*, vol. 2, pp. 4-7, (2014).
- [76] M. D. K. P. V. R. KOLLI<sup>3</sup>, "CHARACTERIZATION AND ANTIBACTERIAL ACTIVITY OF ZnO NANOPARTICLES SYNTHESIZED BY CO PRECIPITATION METHOD," Nov-Dec 2018.
- [77] D. C. Marcano, D. V. Kosynkin, J. M. Berlin, A. Sinitskii, Z. Sun, A. Slesarev, *et al.*, "Improved synthesis of graphene oxide," *ACS nano*, vol. 4, pp. 4806-4814, (2010).
- [78] K. A. Wanderley, A. M. Leite, G. Cardoso, A. M. Medeiros, C. L. Matos, R. C. Dutra, *et al.*, "Graphene oxide and a GO/ZnO nanocomposite as catalysts for epoxy ring-opening of epoxidized soybean fatty acids methyl esters," *Brazilian Journal of Chemical Engineering*, vol. 36, pp. 1165-1173, (2019).
- [79] T. Deosarkar, N. Chandrasekaran, and A. Mukherjee, "An ultra-sensitive and selective AChE based colorimetric detection of malathion using silver nanoparticle-graphene oxide (Ag-GO) nanocomposite," *Analytica Chimica Acta*, vol. 1142, pp. 73-83, (2021).
- [80] V. H. Tran Thi, T. N. Pham, T. T. Pham, and M. C. Le, "Synergistic adsorption and photocatalytic activity under visible irradiation using Ag-ZnO/GO nanoparticles derived at low temperature," *Journal of Chemistry*, vol. (2019), 2019.
- [81] J. H. Kim, H. Park, and S. W. Seo, "In situ synthesis of silver nanoparticles on the surface of PDMS with high antibacterial activity and biosafety toward an implantable medical device," *Nano Convergence*, vol. 4, p. 33, (2017).

- [82] V. A. T. Thi Anh Tuyet Pham, 1 Van Duong Le,1 Minh Viet Nguyen,2 Duc Duc Truong,1 Xuan Truong Do,1 and Anh-Tuan Vu, "Facile Preparation of ZnO Nanoparticles and Ag/ZnO Nanocomposite and Their Photocatalytic Activities under Visible Light," *International Journal of Photoenergy*, vol. 2020, p. 14, (2020).
- [83] S. W. J. W. a. Y. X. L. Q. H. Z. Lu1, "Antibacterial activity and mechanism of Ag/ZnO nanocomposite against anaerobic oral pathogen *Streptococcus mutans*," *Biomaterials synthesis and characterization*, (2017).
- [84] a. B. J. a. A. J. Mahmoud Nasrollahzadeh, "Synthesis, characterization and catalytic activity of graphene oxide/ZnO nanocomposites," *RSC advances*, (2014).
- [85] M. Ana Carolina Mazarin de , Bruna Araujo Lima2,Andreia Fonseca de Faria1,Marcelo Brocchi2,Oswaldo Luiz Alves1, "Graphene oxide-silver nanocomposite as a promising biocidal agent against methicillin resistant *Staphylococcus aureus*," *International Journal of Nanomedicine*, (2015).
- [86] R. G. Nthambeleni Mukwevhoa, c, Elvis Fosso-Kankeua,\*, Neeraj Kumarb, Frans Waandersa, Suprakas Sinha Rayb,c, "Removal of naphthalene from simulated wastewater through adsorption-photodegradation by ZnO/Ag/GO nanocomposite," *Journal of Industrial and Engineering Chemistry*, (2019).
- [87] P. G. C. P. M. Chinnadurai, "Facile synthesis of GO/ZnO–Ag nanocomposite and evaluation of rhodamine B dye under sun light," (2017).
- [88] V. K. Pandey, K. R. Srivastava, G. Ajmal, V. K. Thakur, V. K. Gupta, S. N. Upadhyay, *et al.*, "Differential susceptibility of catheter biomaterials to biofilm-associated infections and their remedy by drug-encapsulated eudragit RL100 nanoparticles," *International journal of molecular sciences*, vol. 20, p. 5110, (2019).
- [89] Y. Yuan, M. P. Hays, P. R. Hardwidge, and J. Kim, "Surface characteristics influencing bacterial adhesion to polymeric substrates," *RSC advances*, vol. 7, pp. 14254-14261, (2017).
- [90] K. Ahmad, R. Noor, M. Younus, A. Chohan, H. M. Asif, and A. W. Chishti, "Green Synthesis and Characterization of Silver Nanoparticles using Crude Extract of *Crotalaria burhia*," *RADS Journal of Pharmacy and Pharmaceutical Sciences*, vol. 8, (2020).
- [91] R. Krishnan, V. Arumugam, and S. K. Vasaviah, "The MIC and MBC of silver nanoparticles against *Enterococcus faecalis*-a facultative anaerobe," *J Nanomed Nanotechnol*, vol. 6, p. 285, (2015).
- [92] A.-L. Kubo, I. Capjak, I. V. Vrček, O. M. Bondarenko, I. Kurvet, H. Vija, *et al.*, "Antimicrobial potency of differently coated 10 and 50 nm silver nanoparticles against clinically relevant bacteria *Escherichia coli* and *Staphylococcus aureus*," *Colloids and Surfaces B: Biointerfaces*, vol. 170, pp. 401-410, (2018).

- [93] P. Parvekar, J. Palaskar, S. Metgud, R. Maria, and S. Dutta, "The minimum inhibitory concentration (MIC) and minimum bactericidal concentration (MBC) of silver nanoparticles against *Staphylococcus aureus*," *Biomaterial investigations in dentistry*, vol. 7, pp. 105-109, (2020).